

AnisoDipFit

Version 1.1

User Manual

Pablo Rauh Corro

Dinar Abdullin

Olav Schiemann

Bonn 2020

Table of contents

Preface	3
1 Introduction	4
1.1 What is it for?	4
1.2 Geometric model of a spin system	5
1.3 Technical information	6
2 Installation	6
3 Running the program.....	6
3.1 Windows.....	6
3.2 Linux	6
4 Graphical User Interface	7
4.1 Main Components	7
4.2 General Tab	8
4.3 Simulation Tab	9
4.4 Fitting Tab	13
4.5 Error Analysis Tab	16
4.6 File Menu	19
4.7 Plot Toolbar.....	20
5 Output data	21
5.1 Simulation output	21
5.2 Fitting output	22
5.3 Error analysis output	23
6 Examples	24
6.1 Simulation of the dipolar spectra of a low-spin Fe ³⁺ -organic radical spin system	24
6.2 Fitting of the PDS time trace of a low-spin Fe ³⁺ -trityl spin system	26
6.3 Simulation of the dipolar spectra of a high-spin Fe ³⁺ -organic radical spin system	30
6.4 Fitting of the dipolar spectrum of a high-spin Fe ³⁺ -nitroxide spin system	32
7 References	36

Preface

AnisoDipFit Version 1.1 (AnisoDipFit v1.1) is an alternative version of the program AnisoDipFit that adds a graphical user interface (GUI) to the existed console application (AnisoDipFit v1.0). The original version of AnisoDipFit can be found here:

<https://github.com/dinarabdullin/AnisoDipFit>.

This manual describes the working principles and the use of AnisoDipFit v1.1. Many chapters in this manual were adapted from the manual of AnisoDipFit v1.0, with permission from the author.

AnisoDipFit v1.1 has been thoroughly tested on several examples. Should you still encounter a bug or unexpected behavior with the program, please feel free to contact me: pablorauhcorro@yahoo.de.

1 Introduction

1.1 What is it for?

Pulsed electron paramagnetic resonance dipolar spectroscopy (PDS)^[1,2] offers several techniques for measuring the dipolar coupling between electron spin centers. The PDS signal is acquired in the form of a time trace, which is modulated by dipolar frequencies. These frequencies can be obtained from the time trace by applying Fourier transform. For disordered samples, Fourier transform yields a distribution of dipolar frequencies, known also as dipolar spectrum. Importantly, dipolar spectra encode information about the distance between electron spin centers and, in some cases, also their relative orientation. In order to extract this spatial information, specialized algorithms of data analysis are required. In the case of the $S = 1/2$ centers with isotropic g -factors of 2.0023, the PDS data analysis can be done by means of the program DeerAnalysis.^[3] This program is also applicable to $S = 1/2$ centers, which have a small g -anisotropy (difference in g -values smaller than 0.1), such as nitroxide radicals. However, if the g -anisotropy of electron spin centers is significant, DeerAnalysis cannot be applied and alternative algorithms of data analysis are required.

The program AnisoDipFit was developed for the analysis of PDS signals that correspond to spin systems consisting of one isotropic and one anisotropic $S = 1/2$ centers. The mathematical background of this analysis is described in Refs. ^[4–7]. AnisoDipFit supports two operation modes: the simulation mode and the fitting mode. In the simulation mode, the PDS signal is calculated using the pre-defined geometric model of a spin system (see Chapter 1.2) and the spectroscopic parameters of spin centers. In the fitting mode, the geometry of a spin system (see Chapter 1.2) is optimized until the simulated PDS signal provides the best fit to the experimental PDS signal. This optimization procedure is done by means of a genetic algorithm.^[5]

The manual is organized as follows. In the rest of Chapter 1, the geometric model of AnisoDipFit and the technical information about the program are provided. Chapters 2 and 3 describe how one can download and run AnisoDipFit with user data, respectively. Chapter 4 provides a comprehensive description of the GUI of AnisoDipFit. The output of the program is described in Chapter 5. Finally, Chapter 6 provides several examples of using AnisoDipFit for the simulation and fitting of PDS signals.

1.2 Geometric model of a spin system

Since there is an infinite number of possible spin system geometries, it is impossible to describe all spin systems with a single geometric model. Therefore, the AnisoDipFit model of a spin system is limited by the following assumptions:

- 1) The spin system consists of two well-localized electron spin centers denoted as spin A and spin B.
- 2) Both electron spin centers have an effective spin $S = 1/2$. Spin A has an isotropic or almost isotropic g -tensor, whereas spin B has an anisotropic g -factor.
- 3) The reference coordinate system of the model is set to be coincident with the g -tensor axes of spin B. A vector that connects spin A with spin B is described by three spherical coordinates: a length r , a polar angle ξ , and an azimuthal angle φ (Figure 1.1).
- 4) In order to account for the conformational flexibility of the spin system, all three geometric parameters, namely r , ξ , and φ , are allowed to have either a uniform distribution or a normal distribution. In both cases, the distributions are described by two parameters, a mean value and a width (Figure 1.2). In the case of the normal distribution, the standard deviation is used as the width parameter.
- 5) Since the PDS data do not provide enough information about potential correlations between the geometric parameters r , ξ , and φ , the geometric model is simplified by assuming the correlations to be zero.

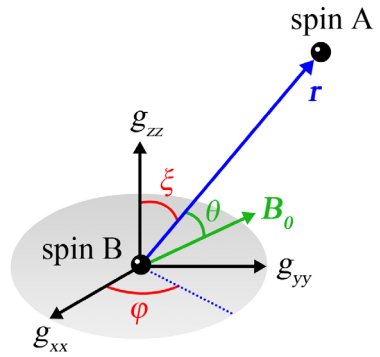


Figure 1.1. The AnisoDipFit model of a spin system.

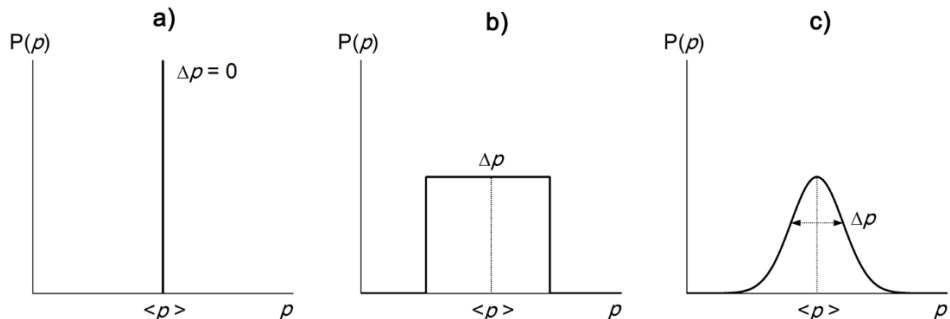


Figure 1.1. The distribution types used for the AnisoDipFit parameter $p \in (r, \xi, \varphi)$. **a)** A single value $\langle p \rangle$. The width Δp equals to 0. **b)** Uniform distribution with the mean value $\langle p \rangle$ and the width Δp . **c)** Normal distribution with the mean value $\langle p \rangle$ and the standard deviation Δp .

1.3 Technical information

AnisoDipFit v1.1 was written in Python 3.7. The source code of the program uses the following libraries: matplotlib (v. 3.2.2), numpy (v. 1.19.0), PyQt5 (v. 5.13.2), scipy (v. 1.5.0), and libconf (v. 2.0.1). The source code can be found at:

[https://github.com/PabloRauhCorro/AnisoDipFit.](https://github.com/PabloRauhCorro/AnisoDipFit)

The Linux and Windows executables of the program can be downloaded from:

[https://github.com/PabloRauhCorro/AnisoDipFit/releases.](https://github.com/PabloRauhCorro/AnisoDipFit/releases)

The program is free of charge and can be distributed under GNU General Public License.

All examples in this manual were tested using a 64-core workstation from sys-Gen GmbH with 2.3 GHz processor frequency and 132 GB RAM.

2 Installation

Download the zip archive with the AnisoDipFit executables at

<https://github.com/PabloRauhCorro/AnisoDipFit/releases>

and unzip it into the directory where the program will be stored. That's all!

3 Running the program

3.1 Windows

Search for the file AnisoDipFit.exe and double click it. Wait a couple of seconds for the program to start.

3.2 Linux

Search for the file AnisoDipFit.exe and double click it. Wait a couple of seconds for the program to start.

- 1) Open the Terminal and navigate into the directory with the program.
- 2) Set the permission properties:

`chmod 755 AnisoDipFit`

`chmod 755 AnisoDipFit.sh`

- 3) Run the program:

`sh AnisoDipFit.sh`

4.1 Main Components

As mentioned in Chapter 1, AnisoDipFit has two main operation modes: simulation and fitting. In the simulation mode, the PDS signal is calculated using the pre-defined geometric model of a spin system (Chapter 4.3). In the fitting mode, the geometric model of a spin system is optimized until the simulated PDS signal provides the best fit to the experimental one (Chapter 4.4). After the fitting, the precision of an optimized geometric model and its parameters is estimated through the error analysis (Chapter 4.5). The structure of the AnisoDipFit GUI mirrors the separation of the program into these operation modes. There are four main tabs: a **General** tab, a **Simulation** tab, a **Fitting** tab and an **Error Analysis** tab (Figure 4.1, blue rectangle). The **General** tab provides the input that is required for all three operation modes. Most importantly, experimental data can be specified in this tab. The **Simulation** tab handles the simulation of PDS spectra and PDS time traces. The **Fitting** tab handles the fitting process of experimental PDS data. The **Error Analysis** tab is used to determine the precision of the fitting results. The **Simulation**, **Fitting**, and **Error Analysis** tabs are separated into sub-tabs that will be explained in the following chapters.

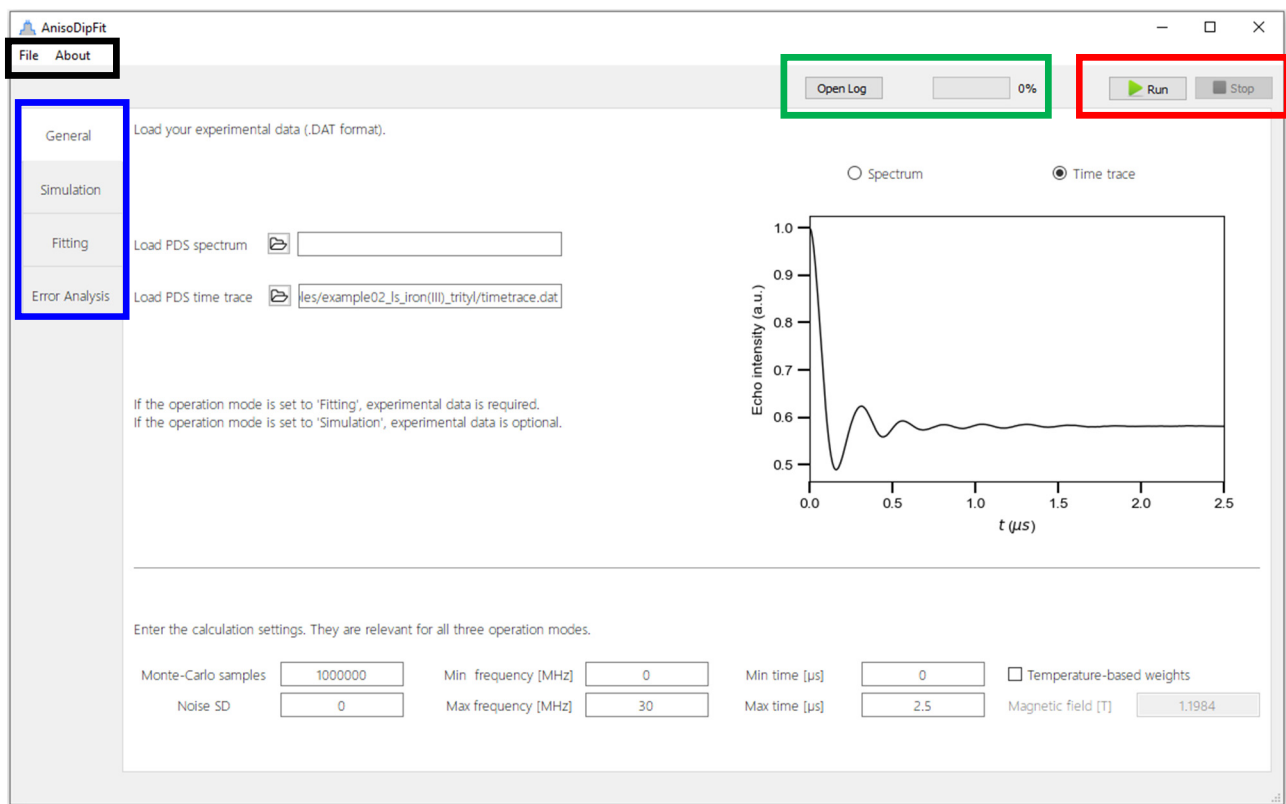


Figure 4.1. Main components of the AnisoDipFit GUI. Black rectangle: **File** and **About** menus. Blue rectangle: Main tabs that define the structure of the GUI. Green rectangle: **Log** button and **Progress Bar**. Red rectangle: **Run** and **Stop** buttons.

Besides the main tabs, the GUI of AnisoDipFit contains the **Run** and **Stop** buttons at the top left corner (Figure 4.1, red rectangle). These buttons are used to run and to terminate the calculations, respectively. The operation mode of AnisoDipFit is determined by the tab from which the user clicks the **Run** button. For example, if the user is currently in the **Simulation** tab and clicks the **Run** button, the program will perform the simulation process. Terminating the calculations with the **Stop** button is not reversible.

Additionally, there is a **File** menu that can be used to save or load data (Figure 4.1, black rectangle) and a progress bar that displays the progress of calculations (Figure 4.1, green rectangle). A log window in the progress bar can be opened with the corresponding button (Figure 4.1, green rectangle). This window contains a list of the performed tasks and their progress.

4.2 General Tab

The **General** tab (Figure 4.2) is used to provide input information that is (in most cases) needed for one of the operation modes of AnisoDipFit.

Experimental data, which can be analyzed by AnisoDipFit, can be either the background-free PDS time trace or the PDS spectrum. This data can be provided by pressing the button with the file icon. The user can then search for the experimental data in his directories. Note that AnisoDipFit only accepts files that have .txt or .dat format. After loading, the experimental data will be shown in a plot on the right-hand side of the **General** tab. In addition, the user can edit several calculation settings:

Monte-Carlo samples	The number of Monte-Carlo samples used in numerical integration. It determines how accurately the PDS time trace or the PDS spectra will be simulated. ^[7] Therefore, it has a strong influence on the runtime of the program. Setting this value below 10^5 heavily reduces the quality of the results.
Noise SD	Standard deviation of noise. It is used to calculate the goodness of fit, χ^2 . If not known, the standard deviation of noise should be set to 0. In this case, the standard deviation of noise will be estimated by the program automatically using the best fit to the experimental data as a reference noise-free signal.
Min frequency	The minimal frequency of the PDS spectrum. Given in [MHz].
Max frequency	The maximal frequency of the PDS spectrum. Given in [MHz]. When an experimental PDS spectrum is loaded, this parameter will be automatically set to the maximum frequency of the spectrum. This parameter can then still be changed.
Min time	The minimal time value of the PDS time trace. Given in [μ s].
Max time	The maximal time value of the PDS time trace. Given in [μ s]. When an experimental PDS time trace is loaded, this parameter will be automatically set to the maximum time value of the time trace. This parameter can then still be changed.
Temperature-based weights	If turned on, the program takes the difference in spin polarization for the different g-values of Spin B into account. This is relevant only for RIDME data acquired at liquid helium temperature. ^[5]

Magnetic Field

The value of the applied magnetic field used in the PDS experiment. Given in [T]. This parameter needs to be provided only if the option [Temperature-based weights](#) is activated.

By default, the presets of all these parameters can be used.

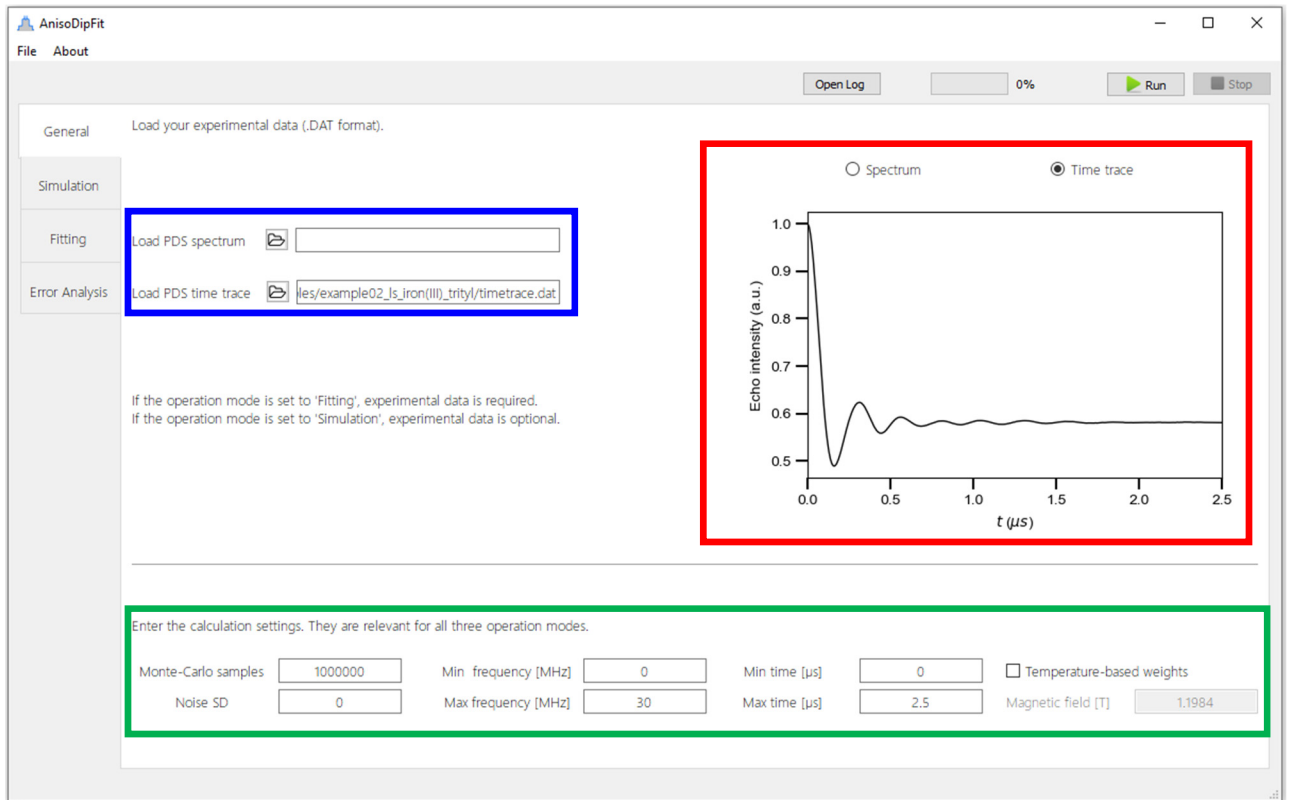


Figure 4.2. General tab. Blue rectangle: Experimental data. Red rectangle: The plot of experimental data. Green rectangle: General settings that are needed for all three operation modes.

4.3 Simulation Tab

The [Simulation](#) tab is separated into three sub-tabs. In the [Input](#) sub-tab, the user chooses the type data the program should simulate. Parameters of the simulation process are defined in this sub-tab too. In the [Spin System](#) sub-tab, the spectroscopic parameters of the spin system are provided. In the [Output](#) sub-tab, the output of the simulation process is displayed.

First, the [Input](#) sub-tab (Figure 4.3) will be considered. It allow the user to choose different types of data that can be simulated:

Time trace Simulate the dipolar time trace. The time ranges will be set according to the values of [Min time](#) and [Max time](#) in the [General](#) tab.

Spectrum Simulate the dipolar spectrum. The frequency ranges will be set according to the values of [Min frequency](#) and [Max frequency](#) in the [General](#) tab.

Spectrum vs θ	Simulate the dipolar spectrum in dependence of the angle θ between the inter-spin vector \vec{r} and the direction of the applied magnetic field \vec{B}_0 (Figure 1.1).
Spectrum vs φ	Simulate the dipolar spectrum in dependence of the angle φ between the projection of the inter-spin vector \vec{r} on the xy -plane of spin B and the g_{xx} -axis of spin B (Figure 1.1).
Spectrum vs ξ	Simulate the dipolar spectrum in dependence of the angle ξ between the inter-spin vector \vec{r} and the g_{zz} -axis of spin B (Figure 1.1).
Spectrum vs T	Simulate the dipolar spectrum in dependence of temperature. This dependence is relevant only for RIDME data acquired at liquid helium temperatures. ^[4]

Moreover, the simulation parameters need to be specified the **Input** sub-tab (Figure 4.3):

$P(r)$, $\langle r \rangle$, Δr	These parameters determine the inter-spin distance distribution $P(r)$. The shape of the distribution $P(r)$ can be either “uniform” or “normal” (Figure 1.2). $\langle r \rangle$ and Δr are the mean value and the width of $P(r)$. Given in [nm].
$P(\varphi)$, $\langle \varphi \rangle$, $\Delta \varphi$	These parameters determine the angular distribution $P(\varphi)$. The shape of the distribution $P(\varphi)$ can be “uniform” or “normal” (Figure 1.2). $\langle \varphi \rangle$ and $\Delta \varphi$ are the mean value and the width of $P(\varphi)$. Given in [°].
$P(\xi)$, $\langle \xi \rangle$, $\Delta \xi$	These parameters determine the angular distribution $P(\xi)$. The shape of the distribution $P(\xi)$ can be “uniform” or “normal” (Figure 1.2). $\langle \xi \rangle$ and $\Delta \xi$ are the mean value and the width of $P(\xi)$. Given in [°].
Min θ, Max θ,	Defines the θ -axis for the Spectrum vs θ simulation. This axis is defined by three numbers, $(\theta_{min}, \theta_{max}, N_\theta)$, where θ_{min} and θ_{max} are the minimal and maximal values of θ , respectively, and N_θ is the number of evenly spaced samples in the interval $[\theta_{min}, \theta_{max}]$.
Number of samples	
Min φ, Max φ,	Defines the φ -axis for the Spectrum vs φ simulation. This axis is defined by three numbers, $(\varphi_{min}, \varphi_{max}, N_\varphi)$, where φ_{min} and φ_{max} are the minimal and maximal values of φ , respectively, and N_φ is the number of evenly spaced samples in the interval $[\varphi_{min}, \varphi_{max}]$.
Number of samples	
Min ξ, Max ξ,	Defines the ξ -axis for the Spectrum vs ξ simulation. This axis is defined by three numbers, $(\xi_{min}, \xi_{max}, N_\xi)$, where ξ_{min} and ξ_{max} are the minimal and maximal values of ξ , respectively, and N_ξ is the number of evenly spaced samples in the interval $[\xi_{min}, \xi_{max}]$.
Number of samples	
Min Temperature,	Defines the temperature-axis (T -axis) for the Spectrum vs T simulation. This axis is defined by three numbers, (T_{min}, T_{max}, N_T) , where T_{min} and T_{max} are the minimal and maximal values of T , respectively, and N_T is the number of evenly spaced samples in the interval $[T_{min}, T_{max}]$.
Max Temperature,	
Number of samples	
Temperature	Temperature of the PDS experiment in [K]. Only relevant for the simulation mode Spectrum vs T . Do not set this parameter to 0!

Modulation depth The modulation depth of the simulated time trace. It needs to be given when the simulation of the time trace is checked and no experimental time trace was defined.

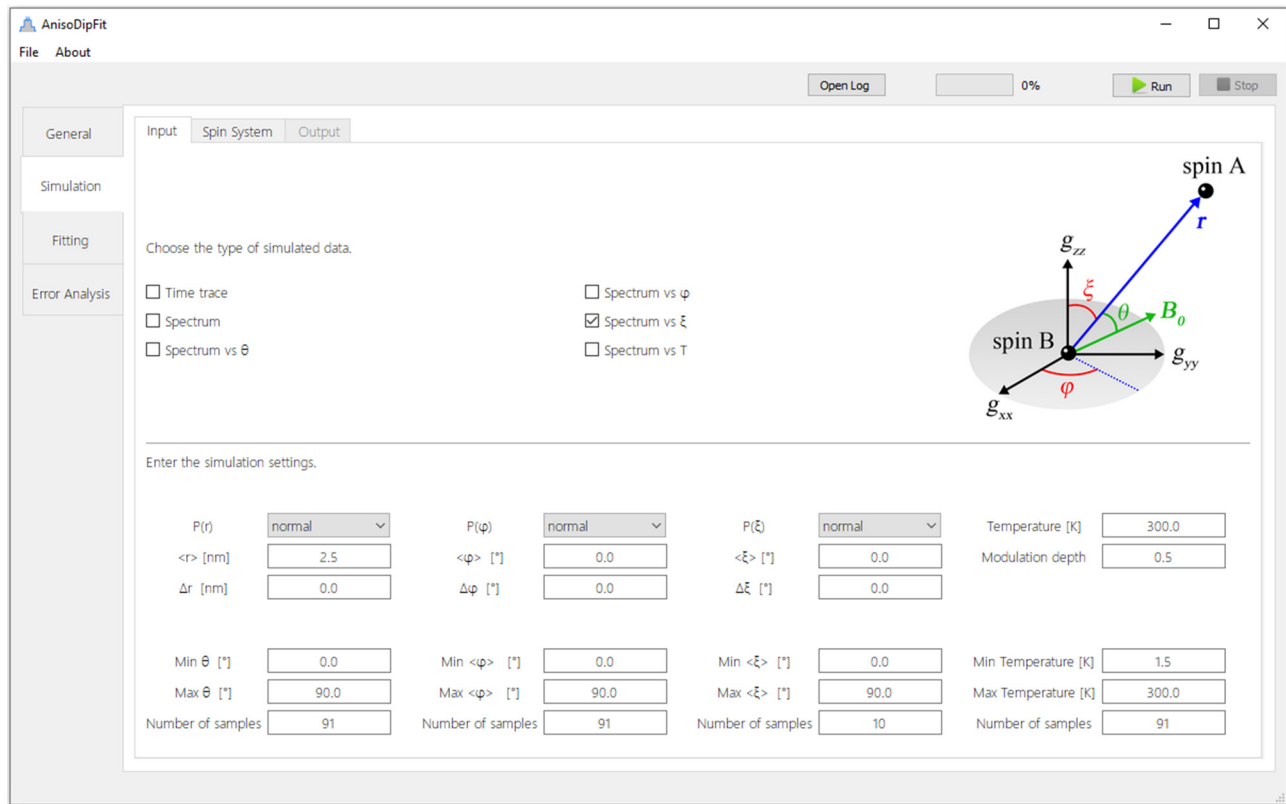


Figure 4.3. Input sub-tab of the Simulation tab.

The spectroscopic parameters of the spin system are provided in the **Spin System** sub-tab. A spin system, which can be considered in AnisoDipFit, consists of two $S = 1/2$ centers denoted as **spinA** and **spinB** (Chapter 1.2). Currently, **spinA** can have only an isotropic or almost isotropic g -tensor, whereas the g -tensor of **spinB** can also be anisotropic.

type

The type of an electron spin center: “isotropic” or “anisotropic”.

g-factor

The g factors contain 3 components: $\mathbf{g} = [g_{xx}, g_{yy}, g_{zz}]$ in the case of an orthorhombic g -factor, $\mathbf{g} = [g_{\perp}, g_{\perp}, g_{\parallel}]$ in the case of an axial g -factor, $\mathbf{g} = [g_{iso}, g_{iso}, g_{iso}]$ in the case of an isotropic g -factor.

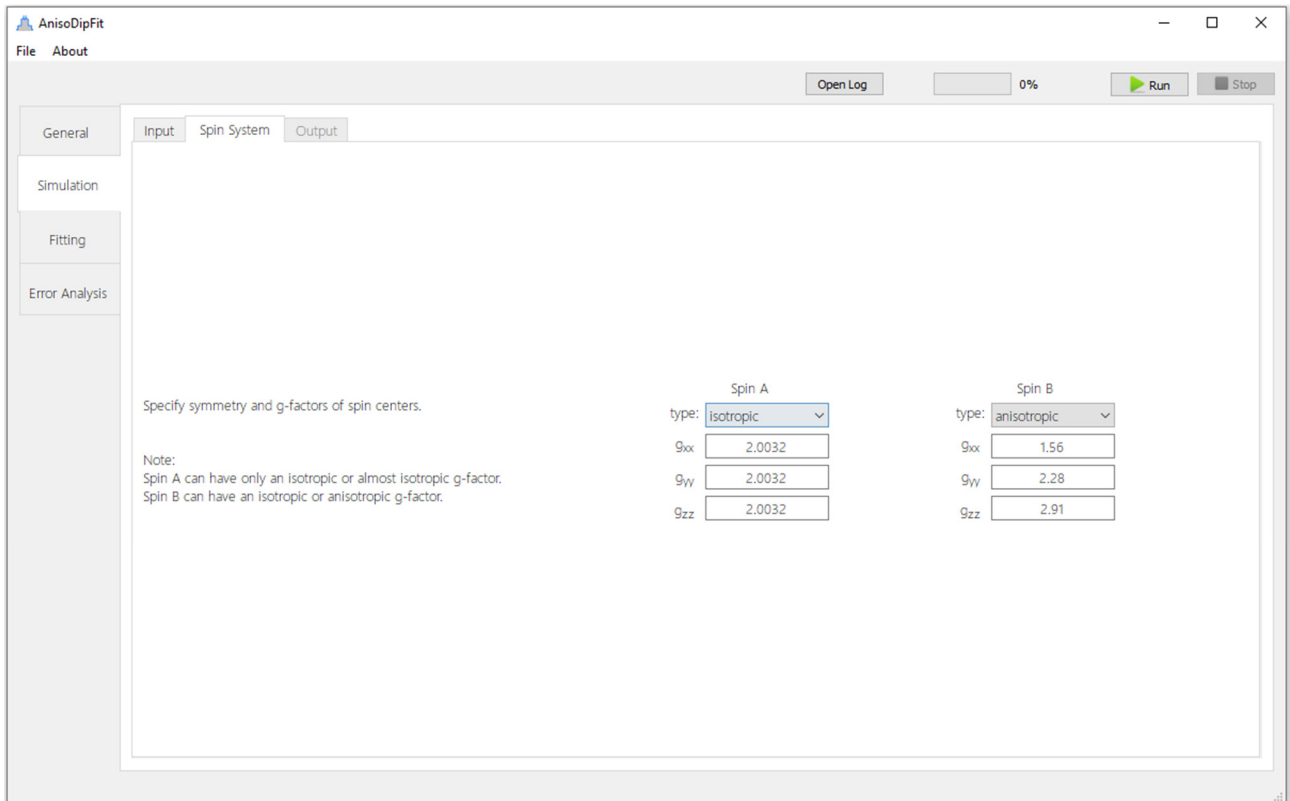


Figure 4.4. Spin System sub-tab of the Simulation tab.

The results of the simulations are displayed in the Output sub-tab. This tab will be available when the simulation is finished. If multiple types of data were simulated, one can use the list on the top left of the tab to switch between the results. Clicking the Normalize frequency axis button will normalize the frequency axis of the displayed spectra to the dipolar coupling constant of an isotropic spin pair,

$$\nu_0 = \frac{\mu_0 \beta_e^2 g_e^2}{4\pi r^3},$$

where μ_0 is the vacuum permeability, β_e is the Bohr magneton, g_e is the g-factor of free electron, and r is set to the value of $\langle r \rangle$. If an experimental spectrum was provided, this option will not be available.

By clicking the 3D-plot button, the results of the Spectrum vs ϕ , Spectrum vs ξ , and Spectrum vs T simulations will be depicted as 3-dimensional plots.

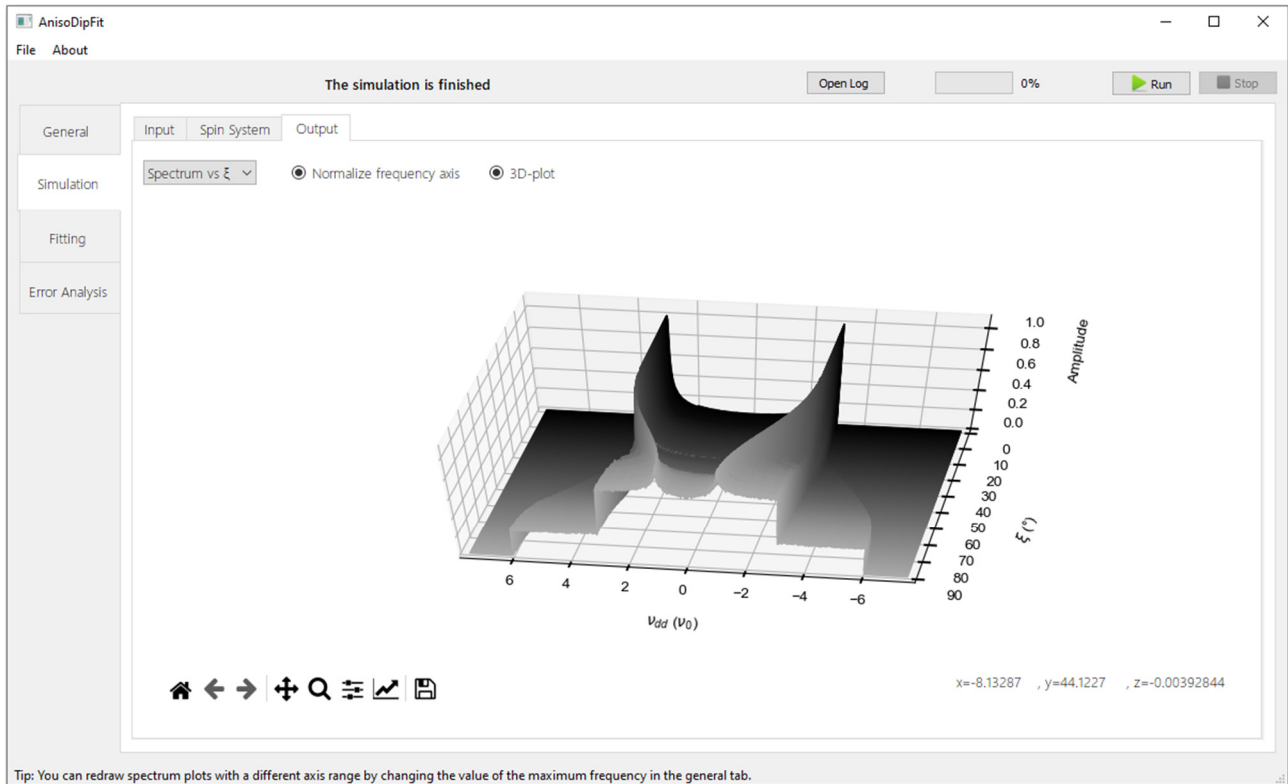


Figure 4.5. [Output](#) sub-tab of the [Simulation](#) tab.

4.4 Fitting Tab

In analogy to the [Simulation tab](#), the [Fitting](#) tab consists of an [Input](#) sub-tab, a [Spin System](#) sub-tab and an [Output](#) sub-tab.

The [Input](#) sub-tab (Figure 4.6) contains information about the type of fitted data, the fitting algorithm, and the fitting parameters. First, the user needs to choose the type of fitted data, which is either an experimental PDS spectrum and an experimental PDS time trace (both are specified in the [General](#) tab). Next, the fitting algorithm has to be specified. Currently, AnisoDipFit allows using only one optimization algorithm, namely the genetic algorithm. This algorithm has been shown to be very efficient when one deals with a large number of optimization parameters and needs to find a global minimum.^[8–11] Importantly, the genetic algorithm has its own internal parameters, which determine its ability to find a global minimum. Optimal values of these parameters may vary depending on a particular PDS data set. Therefore, these parameters can be edited by the user. Pressing the [Edit algorithm parameters](#) will open up a window in which the parameters can be changed. Note that it is highly recommended to use the genetic algorithm's parameters from the configuration files given in the “examples” folder, because these parameters were obtained after extensive tests of the genetic algorithm on numerous PDS data sets. Lastly, the user needs to choose the fitting parameters. These might include the mean values and the widths of the distributions $P(r)$, $P(\phi)$ and $P(\zeta)$, as well as the temperature of the PDS experiment (Table 4.1). The [Optimize](#) checkboxes can be used to include or exclude the corresponding parameters into/from the fitting. The [Lower bound](#) and [Upper bound](#) text fields define the ranges in which the

chosen fitting parameters will be optimized. If some of the parameters should not be optimized, they can be set to a constant values, which are in the **Value** fields. In addition, the distribution types of $P(r)$, $P(\phi)$ and $P(\xi)$ (normal or uniform, see Figure 1.1) can be also selected here.

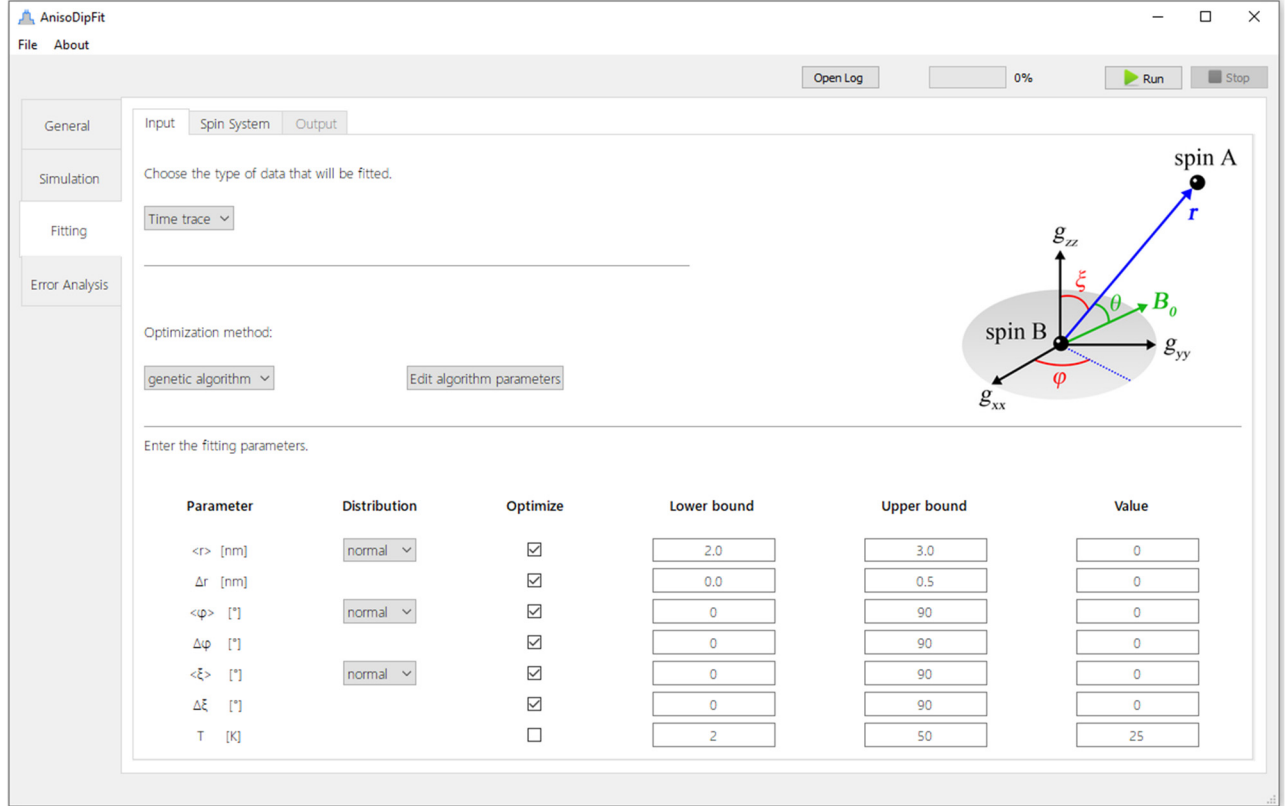


Figure 4.6. Input sub-tab of the Fitting tab.

Table 4.1. The fitting parameters of AnisoDipFit.

Parameter keyword	Parameter description ^[a]	Ranges	Units
$\langle r \rangle$	The mean value $\langle r \rangle$ of the inter-spin distance distribution $P(r)$	Any reasonable ranges	nm
Δr	The width Δr of the inter-spin distance distribution $P(r)$	Any reasonable ranges	nm
$\langle \xi \rangle$	The mean value $\langle \xi \rangle$ of the angular distribution $P(\xi)$	[0, 90]	degree
$\Delta \xi$	The width $\Delta \xi$ of the angular distribution $P(\xi)$	[0, 90]	degree
$\langle \phi \rangle$	The mean value $\langle \phi \rangle$ of the angular distribution $P(\phi)$	[0, 90]	degree
$\Delta \phi$	The width $\Delta \phi$ of the angular distribution $P(\phi)$	[0, 90]	degree
T ^[b]	The temperature of the PDS experiment	Any reasonable ranges	K

^[a] The type of the distributions $P(r)$, $P(\xi)$, and $P(\phi)$ is specified in the Distribution option.

^[b] This parameter is relevant only for the RIDME data acquired at liquid helium temperatures.^[5]

The spectroscopic parameters of the spin system are provided in the [Spin System](#) sub-tab (Figure 4.7). A spin system, which can be considered in AnisoDipFit, consists of two $S = 1/2$ centers denoted as [spinA](#) and [spinB](#) (Chapter 1.2). Currently, [spinA](#) can have only an isotropic or almost isotropic g-tensor, whereas the g-tensor of [spinB](#) can also be anisotropic.

type

The type of an electron spin center: “isotropic” or “anisotropic”.

g-factor

The g factors contain 3 components: $\mathbf{g} = [g_{xx}, g_{yy}, g_{zz}]$ in the case of an orthorhombic g-factor, $\mathbf{g} = [g_{\perp}, g_{\perp}, g_{\parallel}]$ in the case of an axial g-factor, $\mathbf{g} = [g_{iso}, g_{iso}, g_{iso}]$ in the case of an isotropic g-factor.

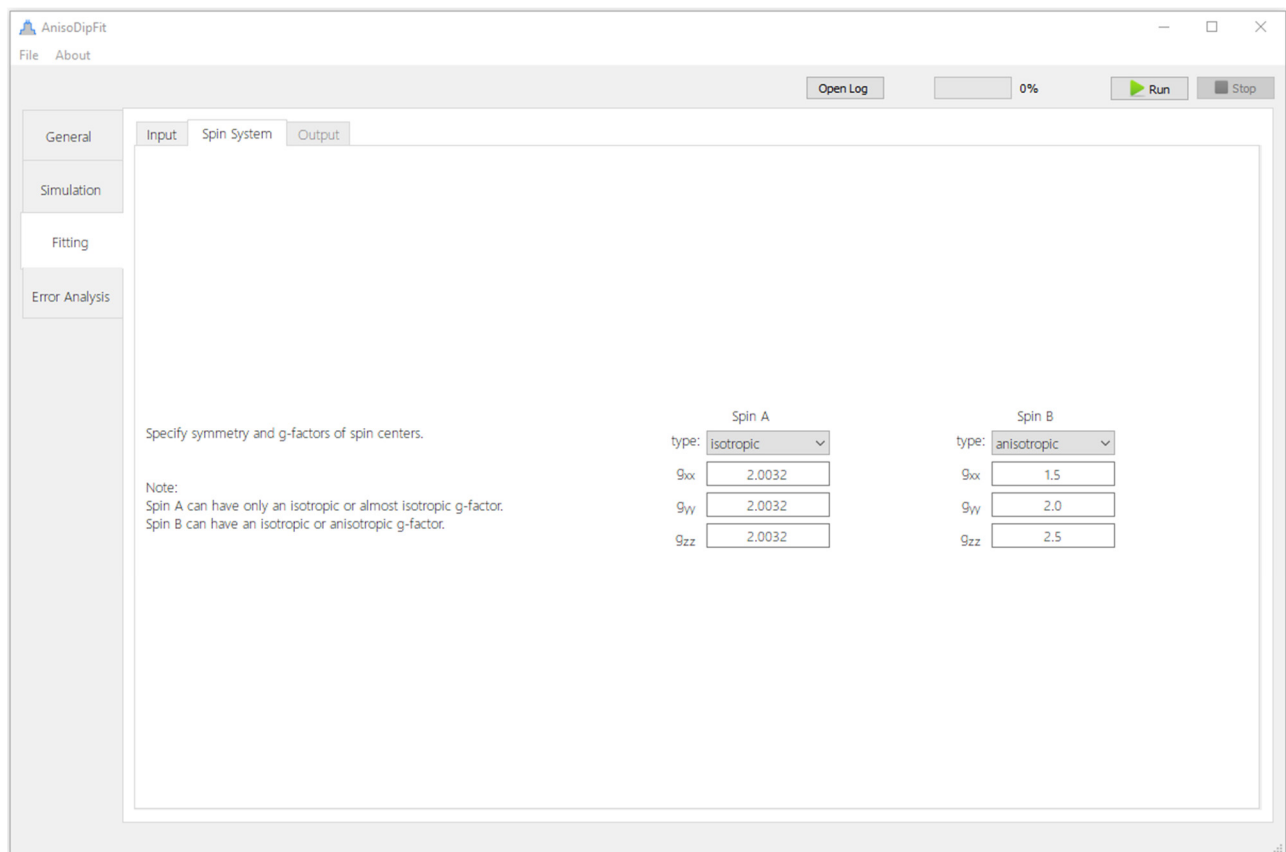


Figure 4.7. [Spin System](#) sub-tab of the [Fitting](#) tab.

The [Output](#) sub-tab (Figure 4.8) is unlocked as soon as the fitting process is started by hitting the [Run](#) button. This tab consists of two plots and a table. The left plot shows the goodness of fit (χ^2) in dependence of the number of optimization steps. The right plot shows both the experimental data and the current best fit. Further discussion of these plots will be done in the Examples chapter. In the table, the optimized values of fitting parameters and their errors (appear only after the error analysis) are listed. Both, the plots and the table, are updated in each optimization steps.

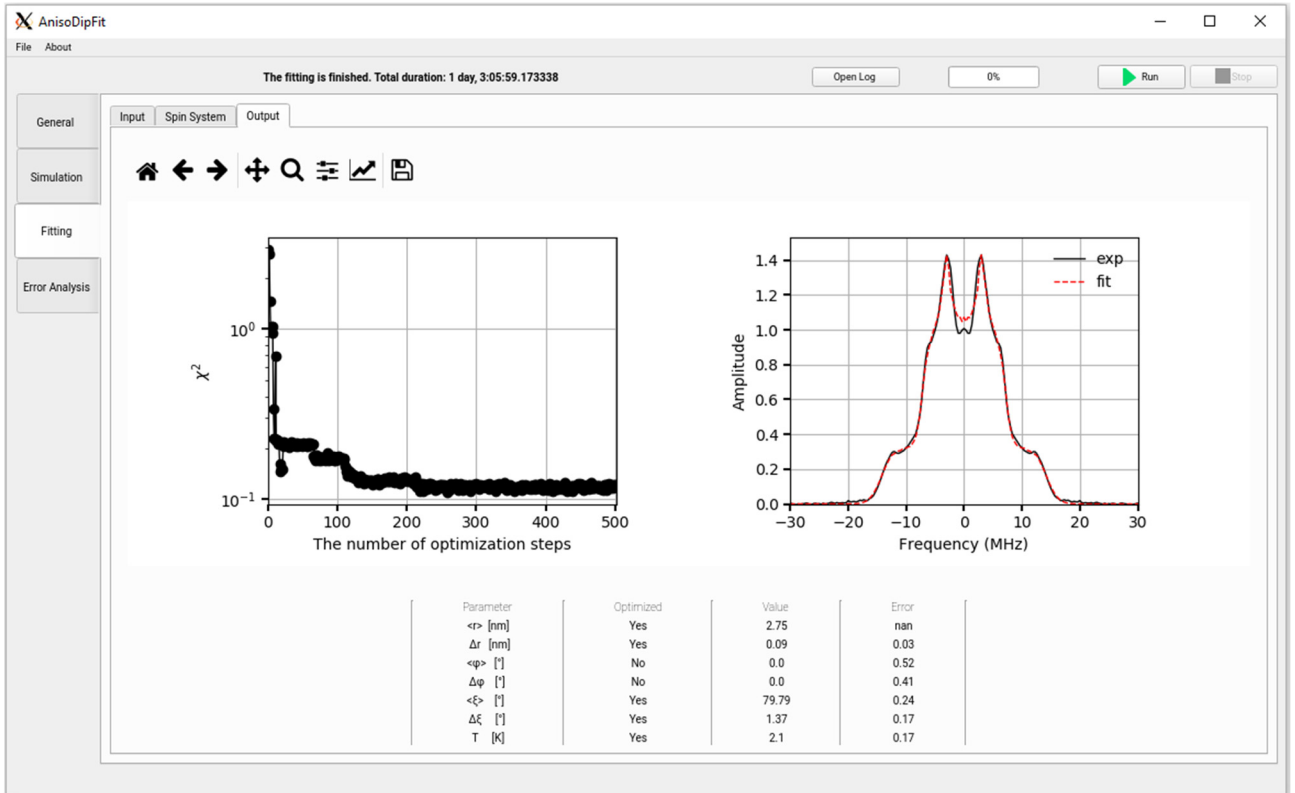


Figure 4.8. Output sub-tab of the Fitting tab.

4.5 Error Analysis Tab

The fitting of PDS data by AnisoDipFit yields the optimized values of fitting parameters, whose precision is unknown. To fill this gap, AnisoDipFit performs an error analysis. Since the parameter space is quite large (up to 7 fitting parameters) and the fitting itself is very time-consuming (hours), usual error analyses, such as bootstrap^[11] and Bayesian analysis^[12], cannot be done within a reasonable time. Therefore, the error analysis is done in a less general way. First, χ^2 is recorded in dependence of $\langle r \rangle$ and Δr , $\langle \zeta \rangle$ and $\Delta \zeta$, $\langle \varphi \rangle$ and $\Delta \varphi$, and T . While recording each of these dependences, the remaining fitting parameters are set to their optimized values. For example, when χ^2 is recorded as a function of $\langle r \rangle$ and Δr , the values of $\langle \zeta \rangle$, $\langle \varphi \rangle$, $\Delta \zeta$, $\Delta \varphi$, and T are fixed at the corresponding optimized values (or at the user-defined values, if some of them were not optimized). Determination of parameters' errors from the obtained dependencies relies on the assumption that the contributions to χ^2 from $P(r)$, $P(\zeta)$, $P(\varphi)$, and T are uncorrelated, at least, near the global minimum. This assumption was confirmed in the previous study,^[6] but in general, it allows to estimate only the lower bound of parameters' uncertainty. Prior to the error estimation, each two-dimensional dependence, e.g. $\chi^2(\langle r \rangle, \Delta r)$, is converted into two one-dimensional dependencies that are optimized with respect to the first or second parameter of the corresponding two-dimensional dependence, e.g. $\chi^2(\langle r \rangle)$ and $\chi^2(\Delta r)$. The obtained one-dimensional dependencies are then used to determine parameter ranges, in which the deviation of the χ^2 values from the minimal χ^2 is less than $\Delta \chi^2$. The threshold $\Delta \chi^2$ is build up out of two contributions. The first contribution, $\Delta \chi_{ci}^2$, takes into account errors related to the noise in the experimental data and possible

discrepancies between the actual spin system and its geometric model. $\Delta\chi_{ci}^2$ is calculated using the user-defined confidence level, e.g. a 3σ confidence level. If one assumes that the measurement errors are distributed normally, $n\sigma$ confidence level corresponds to $\Delta\chi_{ci}^2 = n^2$.^[11] Thus, for the 3σ confidence level one obtains $\Delta\chi_{ci}^2 = 9$. The second contribution, $\Delta\chi_{ne}^2$, takes into account the numerical error, which is mostly determined by the accuracy of the Monte-Carlo integration. The value of $\Delta\chi_{ne}^2$ is estimated by calculating χ^2 for the 10^4 identical sets of optimized fitting parameters and, subsequently, finding the difference between the maximal and minimal values of χ^2 . Lastly, the determined uncertainty ranges are converted into the errors of the fitting parameters by calculating the largest deviation of each parameter from its optimized value within the corresponding uncertainty ranges.

The [Error Analysis](#) tab consists of the three sub-tabs: [Input](#), [Output](#) and [Error Bars](#). In the [Input](#) sub-tab (Figure 4.9), one first needs to specify the fitting data for which the error analysis should be performed. If a fitting process has been performed and the error analysis is now done without having closed the program between fitting and error analysis, these fitting results will be automatically used for error analysis. However, it is also possible to perform the error analysis post-factum. In order to do so, load the file of optimized fitting parameters. This file must have been previously created by saving the results of a fitting process. In addition to this, the following two parameters need to be specified:

Number of points	The number of points in each validation data set. It influences the runtime of the error analysis.
Confidence interval	The confidence interval of fitting parameters in σ units. If one assumes that the measurement errors are distributed normally and the fitting model is linear in its parameters, the 1σ , 2σ , 3σ confidence intervals include the true value of the fitting parameter with the probabilities of 68 %, 95 %, and 99.7 %, respectively.

Lastly, one needs to specify the pairs of parameters for which the dependence of χ^2 will be recorded. By default, the pairs of parameters $\langle r \rangle - \Delta r$, $\langle \zeta \rangle - \Delta \zeta$, and $\langle \varphi \rangle - \Delta \varphi$ will be evaluated. The user can use the combo-boxes at the bottom of the [Input](#) sub-tab to add or remove the parameter pairs.

The [Output](#) (Figure 4.10) and [Error Bars](#) (Figure 4.11) sub-tabs become active after the [Run](#) button was clicked and the error analysis calculations were finished. In the [Output](#) sub-tab, the two-dimensional dependence of χ^2 of parameter pairs are displayed. In the [Error Bars](#) sub-tab, the one-dimensional dependence of χ^2 of single parameters will be shown. These plots will be discussed in detail in the Examples chapter. A distinctive use of the toolbar for error analysis plots is the possibility to change the color coding by choosing a different colormap. This is possible by using the “Edit axis, curve and image parameters” button.

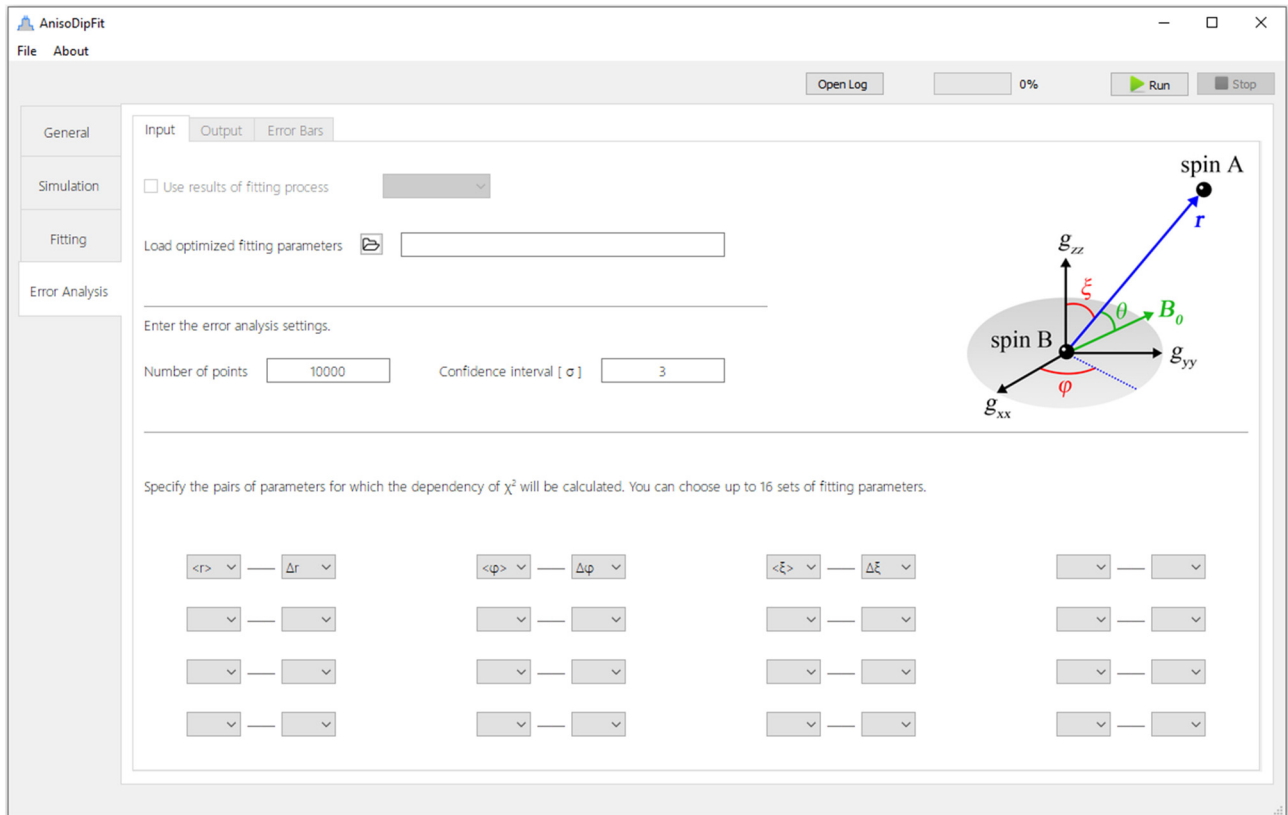


Figure 4.9. Input sub-tab of the Error Analysis tab.

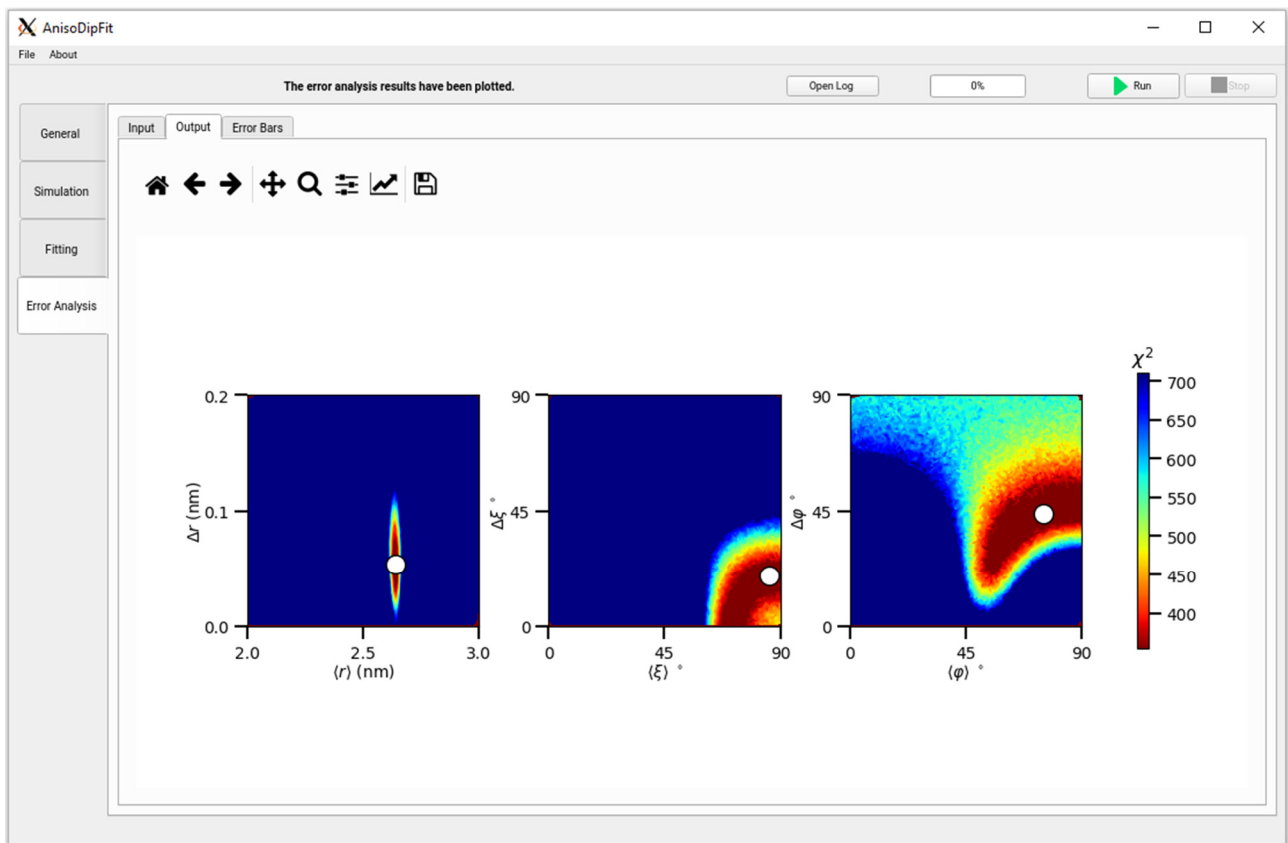


Figure 4.10. Output sub-tab of the Error Analysis tab.

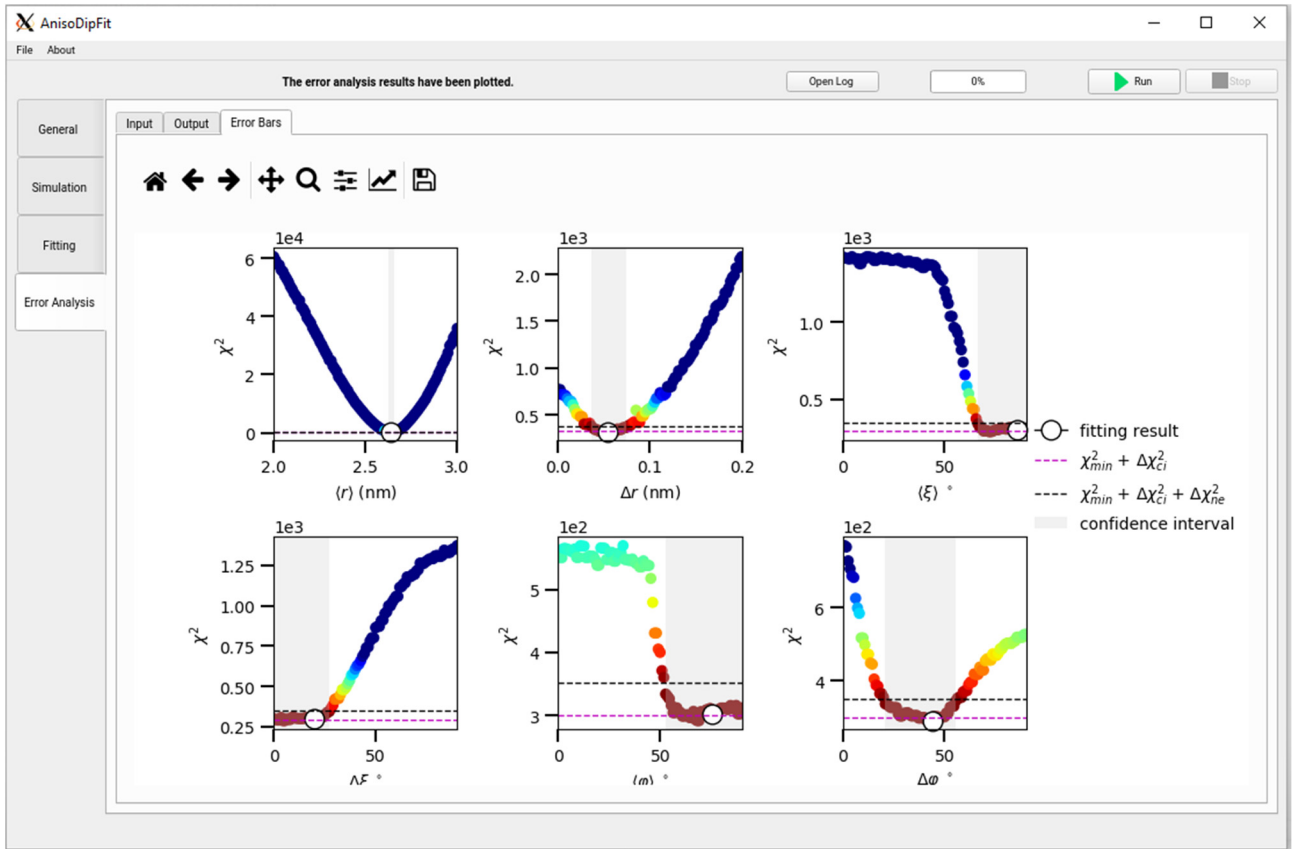


Figure 4.11. Output sub-tab of the Error Analysis tab.

4.6 File Menu

The **File** menu (Figure 4.12) can be found at the top left corner of the GUI. The most important function of the **File** menu is saving the results. To do this, click the corresponding option. In the opened file explorer, choose a directory to save the results in. The output data will be saved as .dat files. The corresponding plots will be saved as .png images. A detailed description of the output data is provided in Chapter 5.

If one wants to run the program multiple times with similar parameters, one can avoid filling in all the input parameters into the GUI several times. Instead, a configuration file, which contains all input parameters of the program, can be saved after the first run and then loaded at any time after that. The detailed description of the configuration can be found at https://github.com/dinarabdullin/AnisoDipFit/blob/master/AnisoDipFit_Manual.pdf (Chapter 4).

The description of all **File** commands is given below:

Save simulation results and plots Save the simulation results into .dat and .png files.

Save fitting results and plots Save the fitting results into .dat and .png files.

Save error analysis results and plots Save the error analysis' results into .dat and .png files.

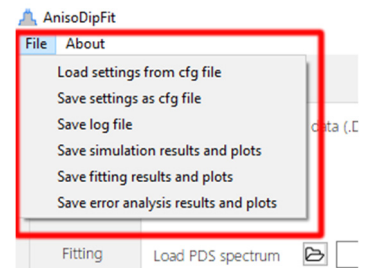


Figure 4.12. The **File** menu.

Save settings as cfg file	Save the configuration file. It stores all input parameters of the program.
Load settings from cfg	Load the configuration file. The program will overwrite all values of the input parameters by the values from the configuration file.
Save log file	Save the content of the Log window.

4.7 Plot Toolbar

All plots in the GUI are accompanied by a **Navigation Toolbar** (from matplotlib, see https://matplotlib.org/3.1.1/users/navigation_toolbar.html). This toolbar provides options such as zooming, panning the axes (for 3d-plots), saving the figure and even editing the figure.

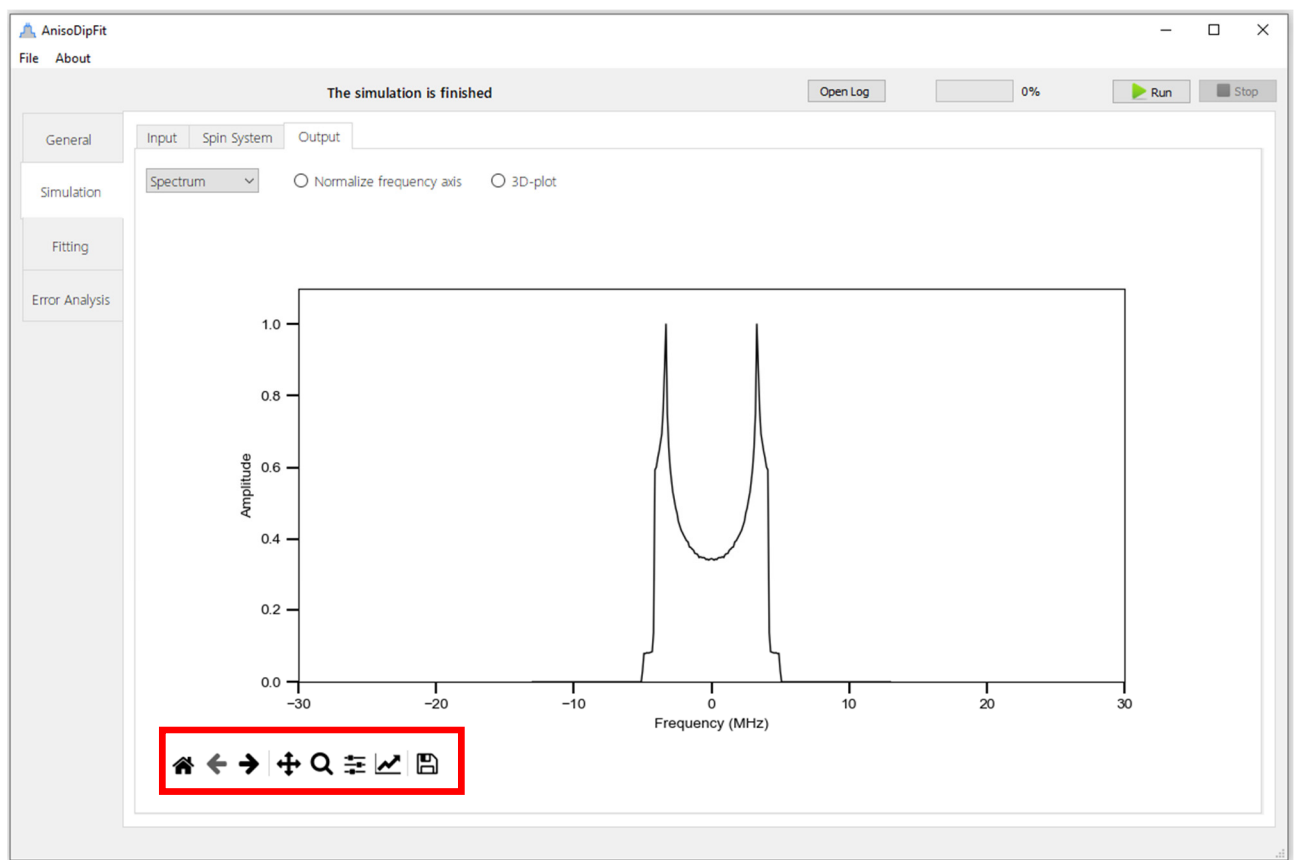


Figure 4.13. Navigation Toolbar.

5 Output data

The output data of AnisoDipFit can be saved by using the corresponding option in the [File](#) menu (Chapter 4.6). The output data is stored in two forms: numerical and graphical. The numerical data is saved as .dat files, whereas the graphical data as .png files. The detailed description of all output files is given below.

5.1 Simulation output

Depending on the simulation settings (Chapter 4.3), the following output files will be created:

- [spc.dat](#)

Data: a simulated dipolar spectrum.
Content: column 1 – frequency values in [MHz];
column 2 – a simulated spectrum;
column 3 – an experimental spectrum (optional).

- [timetrace.dat](#)

Data: a simulated dipolar time trace.
Content: column 1 – time points in [μ s];
column 2 – a simulated time trace;
column 3 – an experimental time trace (optional).

- [spc_vs_X.dat](#), where $X = \text{theta}, \text{xi}, \text{phi}$, or T

Data: dipolar spectra simulated for the different values of parameter X .
Content: column 1 – frequency values in [MHz];
next columns – a spectrum which is simulated with the X value given in the first row of the column.

- [spc.png](#)

Content: the picture of a simulated dipolar spectrum.

- [timetrace.png](#)

Content: the picture of a simulated dipolar time trace.

- [spc_vs_X.png](#), where $X = \text{theta}, \text{xi}, \text{phi}$, or T

Content: the picture of dipolar spectra simulated for the different values of parameter X .

5.2 Fitting output

Depending on the fitting settings (Chapter 4.4), the following output files will be created:

- `score_timetrace.dat` and/or `score_spectrum.dat`

Data: the goodness of fit (χ^2) in dependence of optimization step.

Content: column 1 – optimization steps;

column 2 – χ^2 values.

- `fit_timetrace.dat` and/or `fit_spectrum.dat`

Data: a fit to an experimental PDS time trace or an experimental PDS spectrum.

Content: If `fitted_data = "spectrum"`:

column 1 – frequency values in [MHz];

column 2 – an experimental PDS spectrum;

column 3 – a fit.

If `fitted_data = "timetrace"`:

column 1 – time points in [μ s];

column 2 – an experimental PDS time trace;

column 3 – a fit.

- `optimized_parameters_of_timetrace_fit.dat` and/or `optimized_parameters_of_spectrum_fit.dat`

Data: the optimized values of fitting parameters.

Content: column 1 – the names and the units of fitting parameters;

column 2 – the values of fitting parameters;

column 3 – information about activated (“Y”) and deactivated (“N”) fitting parameters;

column 4 – empty or nan;

5.3 Error analysis output

Depending on the error analysis settings (Chapter 4.5), the following output files will be created:

- [parameters_of_timetrace_fit_with_errors.dat](#) and/or [parameters_of_spectrum_fit_with_errors.dat](#)
Data: the optimized values of fitting parameters.
Content: column 1 – the names and the units of fitting parameters;
column 2 – the values of fitting parameters;
column 3 – information about activated (“Y”) and deactivated (“N”) fitting parameters;
column 4 – the errors of fitting parameters;
- [parameter_errors-X_spectrum.dat](#) and/or [parameter_errors-X_timetrace.dat](#) and/or [parameter_errors-X-Y_spectrum.dat](#) and/or [parameter_errors-X-Y_spectrum.dat](#), where **X** and **Y** are the keywords used for the fitting parameters
Data: the goodness of fit (χ^2) in dependence of fitting parameter(s) **X** (and **Y**)
Content: For one fitting parameter **X**:
column 1 – **X** values;
column 2 – χ^2 values;
For two fitting parameter **X** and **Y**:
column 1 – **X** values;
column 2 – **Y** values;
column 3 – χ^2 values.
- [parameter_errors_spectrum.png](#) and/or [parameter_errors_timetrace.png](#)
Content: the picture of the goodness of fit (χ^2) in dependence of the fitting parameters specified in the [error_analysis](#) list.
- [confidence_intervals_spectrum.png](#) and/or [confidence_intervals_timetrace.png](#)
Content: the picture of the goodness of fit (χ^2) in dependence of single fitting parameters specified in the [error_analysis](#) list.

6 Examples

This chapter provides several examples of how one can use AnisoDipFit to simulate and to fit the PDS data.

6.1 Simulation of the dipolar spectra of a low-spin Fe³⁺-organic radical spin system

The first example deals with the spectral simulations for a spin system consisting of a low-spin Fe³⁺ (ls-Fe³⁺) and an organic radical. The principal *g*-values of the ls-Fe³⁺ are set to $g_{1xx} = 1.56$, $g_{1yy} = 2.28$, and $g_{1zz} = 2.91$. The organic radical is assumed to have an isotropic *g*-factor which is equal to $g_e = 2.0023$. The distance between both spin centers is fixed at 2.50 nm, whereas the values of the ξ and φ angles are varied in the range [0°, 90°] with steps of 10° and 30°, respectively. Thus, the angular dependence of the dipolar spectrum will be explored.

The workflow of this simulation includes the following steps:

- 1) *Run the program.* See Chapter 3 for details.
- 2) *Load the configuration file and run the program.* The configuration file can be loaded by using the corresponding option in the [File](#) menu (Chapter 4.6). The configuration file with all the required settings and parameter values is available in the following directory:

[/AnisoDipFit/examples/example01_ls_iron\(III\)_nitroxide](/AnisoDipFit/examples/example01_ls_iron(III)_nitroxide)

This directory contains four configuration files [config_ex01_i.cfg](#), where $i = 1, 2, 3$, and 4. Each of these configuration files sets up the spectral simulation in dependence of ξ , while setting φ to one of four different values: $\varphi = 0^\circ$ ($i = 1$), $\varphi = 30^\circ$ ($i = 2$), $\varphi = 60^\circ$ ($i = 3$), and $\varphi = 90^\circ$ ($i = 4$).

- 3) *Open the Simulation tab and click the Run button.*
- 4) *Monitor the progress status.* The progress of the simulations is displayed in the progress bar. During the program operation, the following messages should appear in the log bar:

[Starting the simulation...](#)

[Running the pre-calculations...](#)

[Calculating the dipolar spectrum vs xi...](#)

[The simulation is finished.](#)

- 5) *Save the simulation results.* Save the simulation results by using the [Save simulation results and plots](#) option in the [File](#) menu. The following messages will appear in the log window:

[The configuration file has been saved.](#)

[Saving the simulation data...](#)

[The simulation results and graphics have been saved.](#)

- 6) *Explore the simulation results.* The results of simulations will be saved in the folder chosen by the user.

In the given example, the program will create two output files, [spc_vs_xi.dat](#) and [spc_vs_xi.png](#).

Dipolar spectra, obtained from all four simulations, are shown in Figure 6.1. This figure reveals a prominent deviation of the simulated spectra from the Pake doublet.^[14] Whereas the Pake doublet has two characteristic singularities, referred to as perpendicular ($\theta = 90^\circ$) and parallel ($\theta = 0^\circ$) components, all calculated spectra here, display three singularities instead. In analogy to the Pake doublet, these singularities can be subdivided

into two perpendicular components, which correspond to $\theta = 90^\circ$, and one parallel component, which corresponds to $\theta = 0^\circ$. Moreover, the frequencies, at which the singularities appear in Figure 6.1, do not have a fixed ratio, as in the case of the Pake doublet, but depend on the principal g -values of the ls-Fe³⁺ center and the angles ξ and φ . This dependence can be readily explained on example of four spectra corresponding to the angular combinations $(\xi, \varphi) = (0^\circ, 0^\circ), (0^\circ, 90^\circ), (90^\circ, 0^\circ)$ and $(90^\circ, 90^\circ)$. For the angular combination $(0^\circ, 0^\circ)$, the inter-spin vector \vec{r} is collinear to the g_{zz} -axis of the ls-Fe³⁺ g -tensor. Consequently, the parallel component of the spectrum is scaled by g_{zz} , yielding a singularity at $2(g_{zz}/g_e)v_0 \approx 2.91 v_0$. Then, the other two components of the ls-Fe³⁺ g -tensor give rise to two perpendicular components, which appear at $(g_{xx}/g_e)v_0 \approx 0.78 v_0$ and $(g_{yy}/g_e)v_0 \approx 1.14 v_0$. The same assignment of singularities also holds for the spin pair geometry with $(\xi, \varphi) = (0^\circ, 90^\circ)$, because the shape of the dipolar spectrum does not depend on the φ angle as soon as the ξ angle equals 0° . For the angular combination $(90^\circ, 0^\circ)$, \vec{r} is aligned along the g_{xx} -axis of the ls-Fe³⁺ g -tensor. Thus, the parallel component of the spectrum is scaled by g_{xx} and appears at components $2(g_{xx}/g_e)v_0 \approx 1.56 v_0$, whereas two perpendicular components are scaled by g_{yy} and g_{zz} and appear at $(g_{yy}/g_e)v_0 \approx 1.14 v_0$ and $(g_{zz}/g_e)v_0 \approx 1.45 v_0$, respectively. Finally, the angular combination $(90^\circ, 90^\circ)$ corresponds to the case where \vec{r} is collinear to the g_{yy} -axis of the ls-Fe³⁺ g -tensor. In this case, the parallel component of the spectrum is determined by the value of g_{yy} , which yields the singularity at $2(g_{yy}/g_e)v_0 \approx 2.28 v_0$, whereas the perpendicular components of the spectrum are scaled by g_{xx} and g_{zz} and appear at $(g_{xx}/g_e)v_0 \approx 0.78 v_0$ and $(g_{zz}/g_e)v_0 \approx 1.45 v_0$.

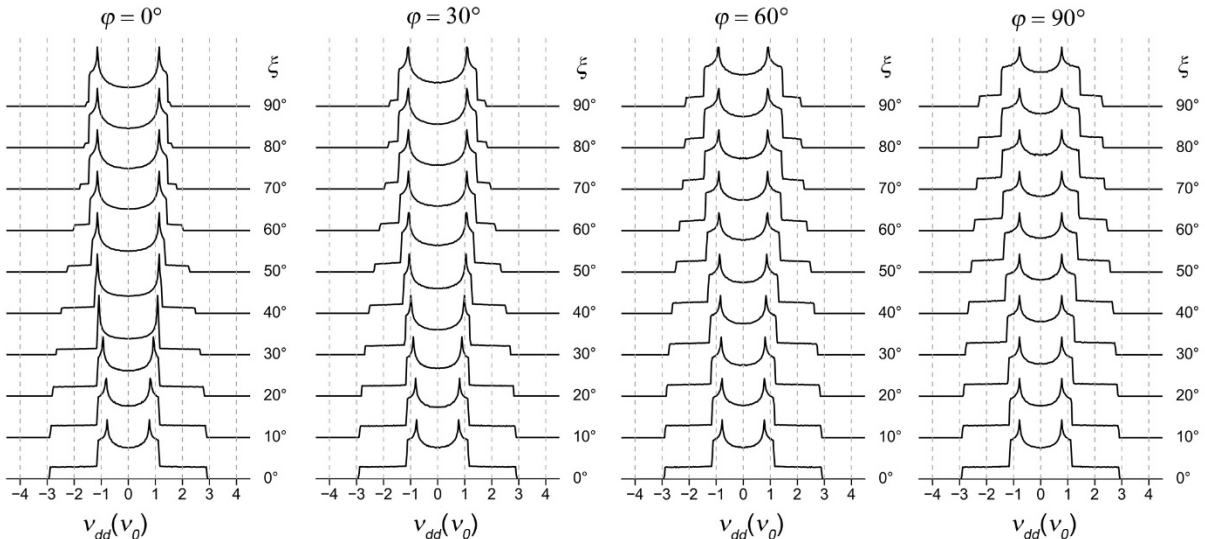


Figure 6.1 The angular dependence of the dipolar spectrum, which corresponds to the spin system consisting of an isotropic organic radical with $g = g_e$ and an anisotropic ls-Fe³⁺ with $g = [1.56, 2.28, 2.91]$. The angles ξ and φ are defined in Figure 1.1.

6.2 Fitting of the PDS time trace of a low-spin Fe³⁺-trityl spin system

In the second example, the fitting and error analysis modes of AnisoDipFit will be explored. The PDS data, which is used for this example, was acquired on the model compound **1**^[6] (Figure 6.2). This compound contains two spatially separated electron spin centers, the trityl radical and the low-spin Fe³⁺ (ls-Fe³⁺). The former spin center has an almost isotropic *g*-factor of 2.0032, whereas the latter one shows a pronounced *g*-anisotropy with three principal components $g_{xx} = 1.56$, $g_{yy} = 2.28$, and $g_{zz} = 2.91$. The PDS measurements on **1** were done using the pulse sequence relaxation induced dipolar modulation enhancement (RIDME)^[15,16] and yielded the background-free time trace shown in Figure 6.3b. Here, this time trace will be fitted using the parameters of $P(r)$, $P(\zeta)$, and $P(\phi)$ as fitting parameters.

The workflow of this fitting includes the following steps:

- 1) *Run the program.* See Chapter 3 for details.
- 2) *Load the configuration file and run the program.* The configuration file can be loaded by using the corresponding option in the [File](#) menu (Chapter 4.6). The configuration file with all the required settings and parameter values is available in the following directory:

[/AnisoDipFit/examples/example02_ls_iron\(III\)_trityl](/AnisoDipFit/examples/example02_ls_iron(III)_trityl)

As follows from this configuration file, the RIDME time trace of **1** is going to be fitted. The mean values and the widths of the distributions $P(r)$, $P(\zeta)$, and $P(\phi)$ are set to be the fitting parameters. All three distributions are approximated by normal distributions and, therefore, their widths are given by standard deviations. The genetic algorithm is set to be the fitting method. The total number of optimization steps is set to 500. For the error analysis, the recording of the following data sets is activated: 1) the two-dimensional dependence of χ^2 on $\langle r \rangle$ and Δr ; 2) the two-dimensional dependence of χ^2 on $\langle \zeta \rangle$ and $\Delta \zeta$; and 3) the two-dimensional dependence of χ^2 on $\langle \phi \rangle$ and $\Delta \phi$. Each of these data sets will contain 10^4 data points. The errors of the fitting parameters will be determined at the 3σ level.

- 3) *Open the Fitting tab and click the Run button.*
- 4) *Monitor the progress status.* Monitor the progress status. The progress of the fitting is displayed in the progress bar. During the program operation, the following messages should appear in the log window:
[Initializing the fitting process...](#)
[Fitting...](#)

[The fitting is finished. Total duration: 17:26:27.807848](#)

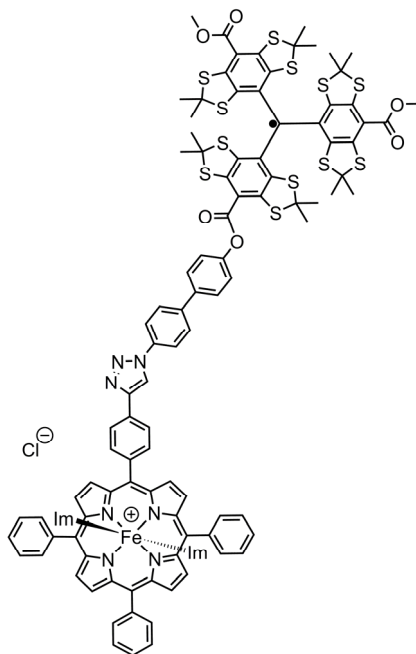


Figure 6.2. The chemical structure of the model compound **1**.

- 5) *Save the fitting results.* Save the fitting results by using the [Save fitting results and plots](#) option in the [File](#) menu. The following messages will appear in the log window:
- [The configuration file has been saved.](#)
- [Saving the fitting data...](#)
- [The fitting results and graphics have been saved.](#)
- 6) *Run the error analysis.* Once the fitting is finished, switch to the [Error Analysis](#) tab and press the [Run](#) button.
- 7) *Monitor the error analysis progress.* Unfortunately, a smooth movement of the progress bar value could not be implemented for the error analysis. Therefore, long lasting periods of the same progress bar value are no reason for concern. During the error analysis, these messages should appear in the log window:
- [Initializing the error analysis...](#)
- [Calculating the dependence of score on fitting parameters...](#)
- [Calculating the errors of fitting parameters...](#)
- [The error analysis is finished. Total duration: 9:29:43.359587](#)
- [Plotting the error analysis results...](#)
- [The error analysis results have been plotted.](#)
- 7) *Save the error analysis results.* Save the results by pressing the [Save error analysis results and plots](#) option in the [File](#) menu. The following messages will appear in the log window:
- [Saving the error analysis results...](#)
- [The error analysis results and graphics have been saved.](#)
- 8) *Explore the results.* The results will have been saved in the user defined folder. The output files of the fitting include [score_timetrace.dat](#), [fit_timetrace.dat](#), [optimized_parameters_of_timetrace_fit.dat](#), and the corresponding graphical files (see Chapter 5.2). The output file of error analysis include [parameter_errors_r_mean-r_width_timetrace.dat](#), [parameter_errors_xi_mean_xi_width_timetrace.dat](#), [parameters_of_timetrace_fit_with_errors.dat](#), and the corresponding graphical files (see Chapter 5.2).

Next, the results of the fitting will be briefly discussed. First, it is important to make sure that the genetic algorithm has converged to the global minimum. This information can be obtained from the output files [score_timetrace.dat](#) and [score_timetrace.png](#), which contain the dependence of χ^2 on the optimization step. In the present fitting, the χ^2 fell gradually down during the first 270 optimization steps and, after this, did not change significantly during the last 230 optimization steps (Figure 6.3a). This reveals that the minimum of the optimization problem was reached. Since the genetic algorithm is capable to find the global minimum even for optimization problems with several local minima, the obtained minimum is most likely global. This is supported by fact that a good fit to the RIDME data was indeed obtained. The fit is stored in the output files [fit_timetrace.dat](#) and [fit_timetrace.png](#) and depicted here in Figure 6.3b. The corresponding optimized values of the fitting parameters are stored in the output file [optimized_parameters_of_timetrace_fit.dat](#). The content of this file is listed in Figure 6.3c. In order to estimate the errors of these parameters, the following data was recorded: 1) the two-dimensional dependence of χ^2 on $\langle r \rangle$ and Δr ([parameter_errors-r_mean-](#)

`r_width_timetrace.dat`), 2) the two-dimensional dependence of χ^2 on $\langle \xi \rangle$ and $\Delta\xi$ (`parameter_errors-xi_mean-xi_width_timetrace.dat`), and 3) the two-dimensional dependence of χ^2 on $\langle \varphi \rangle$ and $\Delta\varphi$ (`parameter_errors-phi_mean-phi_width_timetrace.dat`). The picture of these data sets is stored in the output file `parameter_errors_timetrace.png` and shown here in Figure 6.3d. In this figure, the uncertainty ranges of the fitting parameters are depicted in dark red, and the optimized values of the fitting parameters are depicted by white dots. As expected, all dots appear within the uncertainty ranges mentioned above, meaning that the optimized values of the fitting parameters lay within the corresponding uncertainty ranges. In order to determine the errors of fitting parameters, all three two-dimensional dependencies from Figure 6.3c were transformed into one-dimensional dependencies, which contain the dependence of χ^2 on each single fitting parameter. The one-dimensional dependencies are stored in the output file `confidence_intervals_timetrace.png`, whose content is depicted in Figure 6.3e. As can be seen, all one-dimensional dependencies reveal a single, well-defined minimum. The χ^2 threshold, which was used to determine the uncertainty intervals of the fitting parameters, is depicted by the black dashed line. The errors of individual fitting parameters, which were derived from the uncertainty intervals, are listed Figure 6.3c. The errors of the mean inter-spin distance $\langle r \rangle$ and its standard deviation Δr are ± 0.02 nm and ± 0.03 nm, respectively. The errors of the mean angles $\langle \xi \rangle$ and $\langle \varphi \rangle$ equal to $\pm 21^\circ$ and $\pm 34^\circ$, respectively. The corresponding standard deviations $\Delta\xi$ and $\Delta\varphi$ have similar errors, which equal to $\pm 27^\circ$ and $\pm 32^\circ$, respectively. Taken all that, one can conclude that the AnisoDipFit analysis of the RIDME time trace of **1** allowed determining the distance distribution $P(r)$ with a sub-angstrom precision and the angular distributions $P(\xi)$ and $P(\varphi)$ with a moderate precision of $\sim 30^\circ$. Note that the precision of the angular parameters strongly depends on how anisotropic the g -factor of **spin B** is (in the given example, spin B is the $1s\text{-Fe}^{3+}$). It will be shown in Section 6.4 that the precision of the angular parameters can be significantly increased if spin B has a larger g -anisotropy than the $1s\text{-Fe}^{3+}$.

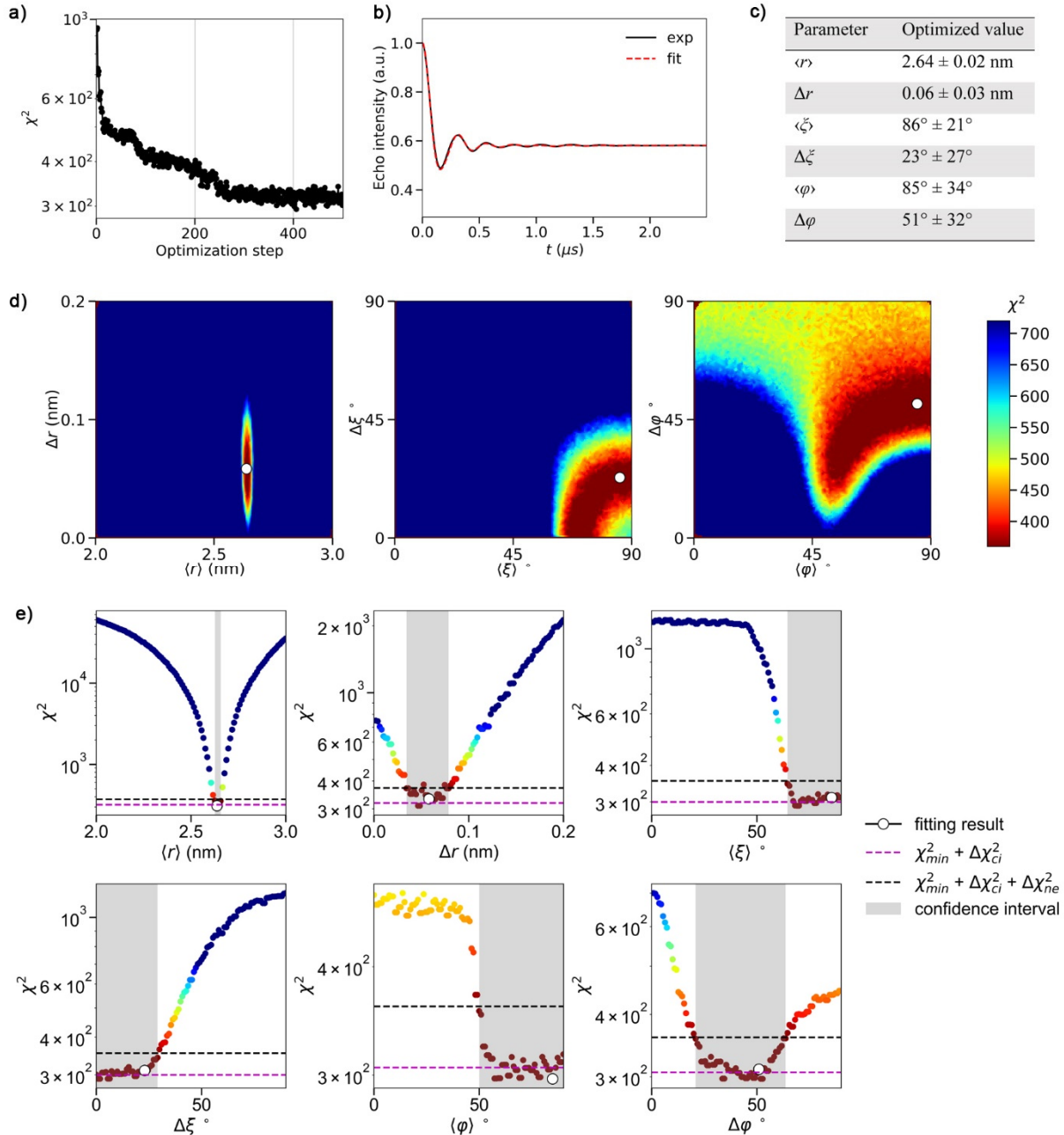


Figure 6.3. Fitting the RIDME time trace of **1** by AnisoDipFit. **a)** The dependence of χ^2 on the optimization step. **b)** The RIDME time trace (black line) is overlaid with the corresponding fit (red line). **c)** The optimized values of the fitting parameters. **d)** The dependence of χ^2 on different pairs of fitting parameters. Dark red regions correspond to the parameters' uncertainty intervals, which lie below the χ^2 threshold. The optimized values of the fitting parameters are depicted by white dots. **e)** The dependence of χ^2 on single fitting parameters. The χ^2 threshold is depicted by the black dashed line. This threshold consists of two contributions, $\Delta\chi_{ci}^2$, which is determined at the 3σ confidence level, and $\Delta\chi_{ne}^2$, which takes into account the numerical error. The uncertainty ranges of the fitting parameters are shown as gray intervals.

6.3 Simulation of the dipolar spectra of a high-spin Fe³⁺-organic radical spin system

In the next example, the simulation mode of AnisoDipFit is used ones again. The spectral simulations are done for a spin system consisting of a high-spin Fe³⁺ (hs-Fe³⁺) and an organic radical. In contrast to the ls-Fe³⁺ considered in Chapter 6.1, the hs-Fe³⁺ has $S = 5/2$ and, therefore, does not satisfy the requirements of AnisoDipFit (Chapter 1.2). However, if the zero-field splitting (ZFS) of the hs-Fe³⁺ significantly exceeds its Zeeman energy and the thermal energy, the hs-Fe³⁺ can be considered an effective $S = 1/2$ center,^[5] which makes AnisoDipFit still applicable. Thus, only this particular case of a large zero-field splitting is considered here. The g-factor of the hs-Fe³⁺ is set to be axial with the principal components $g_{xx} = g_{yy} = 6.0$ (also denoted as g_{\perp}) and $g_{zz} = 2.0$ (also denoted as g_{\parallel}). The g-factor of the organic radical is assumed to be isotropic and equal to $g_e = 2.0023$. In analogy to the example of Chapter 6.1, the inter-spin distance is fixed to 2.50 nm. Due to the axial symmetry of the hs-Fe³⁺ center, the angle φ has no effect on the dipolar spectrum and, therefore, is set to 0°. In contrast, the angle ξ is expected to have an effect on the dipolar spectrum and will be varied in the range [0°, 90°] with a constant step of 0.25°. Additionally, the dipolar spectrum will be simulated in dependence of the angle θ between the inter-spin vector \vec{r} and the direction of the applied magnetic field \vec{B}_0 . The simulation will be done for two particular cases, $\xi = 0^\circ$ and $\xi = 90^\circ$. The idea behind these simulations will become clear later.

The workflow of this fitting includes the following steps:

- 1) *Run the program.* See Chapter 3 for details.
- 2) *Load the configuration file and run the program.* The configuration file can be loaded by using the corresponding option in the [File](#) menu (Chapter 4.6). The configuration file with all the required settings and parameter values is available in the following directory:

[/AnisoDipFit/examples/example03_hs_iron\(III\)_nitroxide](#)

This directory contains three configuration files [config_ex03_i.cfg](#), where $i = 1, 2$, and 3 . The configuration file [config_ex03_1.cfg](#) initializes the spectral simulations in dependence of ξ , whereas the configuration files [config_ex03_2.cfg](#) and [config_ex03_3.cfg](#) initialize the spectral simulations in dependence of θ and set ξ to 0° and 90°, respectively.

- 3) *Open the Simulation tab and click the Run button.*
- 4) *Monitor the progress status.* The progress of the simulations is displayed in the progress bar. During the program operation, the following messages should appear in the log bar:

[Starting the simulation...](#)

[Running the pre-calculations...](#)

[Calculating the dipolar spectrum vs xi... \(Calculating the dipolar spectrum vs theta...\)](#)

[The simulation is finished.](#)

- 5) *Save the simulation results.* Save the simulation results by using the [Save simulation results and plots](#) option in the [File](#) menu. The following messages will appear in the log window:

[The configuration file has been saved.](#)

[Saving the simulation data...](#)

The simulation results and graphics have been saved.

- 6) Explore the simulation results. For the simulation based on [config_ex03_1.cfg](#), the user-defined folder will contain the files [spc_vs_xi.dat](#) and [spc_vs_xi.png](#). For the simulations based on [config_ex03_2.cfg](#) and [config_ex03_3.cfg](#), the user-defined folders will contain the files [spc_vs_theta.dat](#) and [spc_vs_theta.png](#).

As can be seen in Figure 6.4a, the simulated spectra have prominent differences to the Pake doublet.^[14] Firstly, they are significantly broader than the Pake doublet. This stems from the fact that the dipolar coupling frequencies are proportional to the effective g-factors of the hs-Fe³⁺, which are 3 times larger than g_e for two out of three canonical orientations. Secondly, the shapes of the simulated spectra differ from the shape of the usual Pake doublet and, as expected, depend strongly on the angle ξ . In order to provide a deeper insight into the obtained shapes, the dipolar spectrum is plotted as a function of θ for two particular cases, $\xi = 0^\circ$ and $\xi = 90^\circ$. In the case of $\xi = 90^\circ$ (Figure 6.4b), the parallel component ($\theta = 90^\circ$) of the spectrum scales with g_{yy} of the hs-Fe³⁺, which is about 3 times larger than g_e . Consequently, the parallel component appears in the spectrum at $\pm 6v_0$ and not at $\pm 2v_0$ as for the Pake doublet. The perpendicular component ($\theta = 0^\circ$) of the spectrum scales with the g-values of the hs-Fe³⁺ ranging from $g_{zz} \approx g_e$ to $g_{xx} \approx 3g_e$. This gives rise to two features in the spectrum at $\pm v_0$ and $\pm 3v_0$, respectively. In the case of $\xi = 0^\circ$ (Figure 6.4c), the perpendicular component ($\theta = 90^\circ$) of the spectrum scales with g_{xx} and g_{yy} of the hs-Fe³⁺. Since $g_{xx} = g_{yy} \approx 3g_e$, the perpendicular component of the spectrum appears at $\pm 3v_0$. The parallel component ($\theta = 0^\circ$) of this spectrum scales with g_{zz} of the hs-Fe³⁺ and, thus, should appear at $\pm 2v_0$. Since the parallel component has a smaller probability and appears at lower frequencies than the perpendicular component, it does not yield any prominent features in the spectrum.

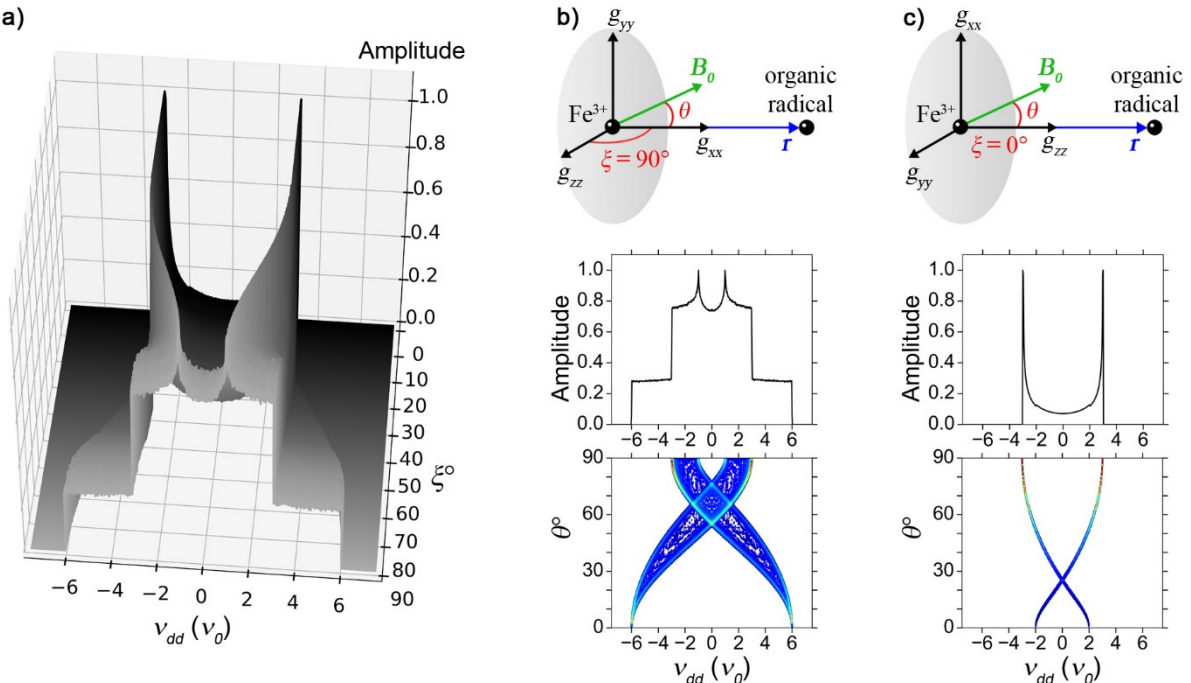


Figure 6.4. a) The angular dependence of the dipolar spectrum that corresponds to the spin system consisting of an isotropic organic radical with $g_{iso} = g_e$ and an anisotropic hs-Fe³⁺ with $g_{aniso} = [6.0, 6.0, 2.0]$. The angle ξ is defined in Figure 1.1. For the particular cases of the b) $\xi = 0^\circ$ and c) $\xi = 90^\circ$, the dipolar spectrum is also shown in dependence of the angle θ . Top: The geometric model of the spin system with the fixed ξ angle. Middle: The corresponding dipolar spectrum. Bottom: The corresponding dipolar spectrum plotted against θ .

6.4 Fitting of the dipolar spectrum of a high-spin Fe³⁺-nitroxide spin system

In the last example, AnisoDipFit is applied to the fitting of a RIDME spectrum acquired on the MTSI-labeled mutant Q8R1 of the hemeprotein met-myoglobin (Figure 6.5).^[5] This met-myoglobin mutant contains two spatially separated electron spin centers, the nitroxide and the high-spin Fe³⁺ (hs-Fe³⁺). The hs-Fe³⁺ has the large axial ZFS ($D \sim 9.26 \text{ cm}^{-1}$, $E = 0.0023 \text{ cm}^{-1}$),^[17] which allows considering this ion as an effective $S = 1/2$ center at Q-band and at the temperatures below 3 K.^[5] The g -factor of this center is very anisotropic and has the principal components $g_{xx} = 5.93$, $g_{yy} = 5.94$, and $g_{zz} = 2.00$. In contrast, the g -anisotropy of the nitroxide center is so small that it can be neglected in the data analysis by setting all g -values to g_e . Since the g -factor of the hs-Fe³⁺ is almost axial, the RIDME spectrum of Q8R1 does not depend

on the angle φ . Therefore, this angle will be excluded from the fitting and fixed at a constant value of 0°. Thus, the fitting of the RIDME spectrum will be done using the parameters of only two distributions, $P(r)$ and $P(\zeta)$, as fitting parameters. In addition, the temperature of the RIDME experiment will be used as a fitting parameter. This has the following reasons: 1) If the Zeeman energy of the hs-Fe³⁺ becomes comparable to the thermal energy, the corresponding RIDME spectrum becomes temperature dependent (for explanation see Ref. [5]). The RIDME measurements on Q8R1 apply to this case. 2) The error of the experimentally measured temperature was above the precision required for accurate spectral simulations.

The workflow of this fitting includes the following steps:

- 1) *Run the program.* See Chapter 3 for details.
- 2) *Load the configuration file and run the program.* The configuration file can be loaded by using the corresponding option in the [File](#) menu (Chapter 4.6). The configuration file with all the required settings and parameter values is available in the following directory:

[/AnisoDipFit/examples/example04_hs_iron\(III\)_nitroxide](#)

As follows from this configuration file, the data, which is going to be fitted, is the RIDME spectrum of Q8R1. The mean values and the widths of the distributions $P(r)$ and $P(\zeta)$, as well as the temperature, are selected to be the fitting parameters. The distributions $P(r)$ and $P(\zeta)$ are approximated by normal distributions and, therefore, their widths are given as standard deviations. The genetic algorithm is set to be the fitting method. The total number of optimization steps is set to 500. For the error analysis, the recording of the following data sets is activated: 1) the two-dimensional dependence of χ^2 on $\langle r \rangle$ and Δr , 2) the two-dimensional dependence of χ^2 on $\langle \zeta \rangle$ and $\Delta \zeta$, and 3) the two-dimensional dependence of χ^2 on

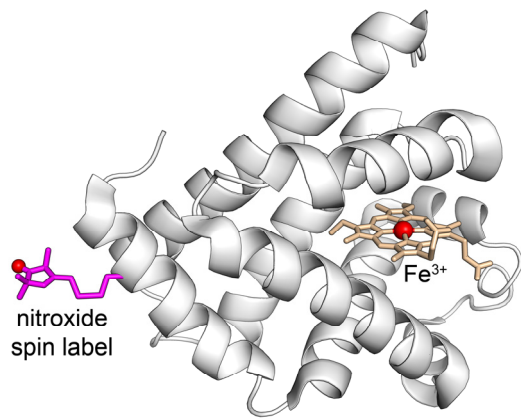


Figure 6.5. The structural model of the met-myoglobin mutant Q8R1. This model is based on the crystal structure of met-myoglobin (PDB-ID 1wla)^[18], which is shown in white. The heme group and the Fe³⁺ ion are depicted as light orange sticks and a red sphere, respectively. A single conformer of the nitroxide spin label, attached at the position Q8, is depicted by magenta sticks. The corresponding oxygen atom is shown as a red sphere.

the temperature. Each of these data sets will contain 10^4 data points. The errors of the fitting parameters will be determined at the 3σ level.

- 3) *Open the Fitting tab and click the Run button.*
- 4) *Monitor the progress status.* The progress of the fitting is displayed in the progress bar. During the program operation, the following messages should appear in the log window:
Initializing the fitting process...
Fitting...
The fitting is finished. Total duration: 16:39:59.540339
- 5) *Save the fitting results.* Save the fitting results by using the [Save fitting results and plots](#) option in the [File](#) menu. The following messages will appear in the log window:
The configuration file has been saved.
Saving the fitting data...
The fitting results and graphics have been saved.
- 6) *Run the error analysis.* Once the fitting is finished, switch to the [Error Analysis](#) tab and press the [Run](#) button.
- 7) *Monitor the error analysis progress.* Unfortunately, a smooth movement of the progress bar value could not be implemented for the error analysis. Therefore, long lasting periods of the same progress bar value are no reason for concern. During the error analysis, these messages should appear in the log window:
Initializing the error analysis...
Calculating the dependence of score on fitting parameters...
Calculating the errors of fitting parameters...
The error analysis is finished. Total duration: 9:16:26.985827
Plotting the error analysis results...
The error analysis results have been plotted.
- 8) *Save the error analysis results.* Save the results by pressing the [Save error analysis results and plots](#) option in the [File](#) menu. The following messages will appear in the log window:
Saving the error analysis results...
The error analysis results and graphics have been saved.

- 8) *Explore the results.* The results will have been saved in the user defined folder. The output files of the fitting include `score_spectrum.dat`, `fit_spectrum.dat`, `optimized_parameters_of_spectrum_fit.dat`, and the corresponding graphical files (see Chapter 5.2). The output file of error analysis include `parameter_errors-r_mean-r_width_spectrum.dat`, `parameter_errors-xi_mean-xi_width_spectrum.dat`, `parameter_errors-temp_spectrum.dat`, and the corresponding graphical files (see Chapter 5.2).

Next, the results of the fitting will be briefly discussed. The discussion will begin by exploring the content of the files `score_spectrum.dat` and `score_spectrum.png`. These files contain the dependence of χ^2 on the optimization step, which is depicted in Figure 6.6a. This figure reveals that χ^2 decreased during first 50 optimization steps and, then, reached a plateau during the next 450 optimization steps. Based on this, one can

conclude that the genetic algorithm has converged to the minimum. The fit to the RIDME spectrum, which corresponds to the obtained minimum, is stored in the output files [fit_spectrum.dat](#) and [fit_spectrum.png](#) and depicted in Figure 6.6b. As can be seen, the shape of the experimental RIDME spectrum is well reproduced by the obtained fit, revealing the minimum that was found by the genetic algorithm is a global minimum. The corresponding optimized values of the fitting parameters are stored in the output file [optimized_parameters_of_spectrum_fit.dat](#), whose content is listed in Figure 6.6c. In order to estimate the errors of these parameters, the following data was recorded: 1) the two-dimensional dependence of χ^2 on $\langle r \rangle$ and Δr ([parameter_errors-r_mean-r_width_spectrum.dat](#)), 2) the two-dimensional dependence of χ^2 on $\langle \xi \rangle$ and $\Delta \xi$ ([parameter_errors-xi_mean-xi_width_spectrum.dat](#)), and 3) the one-dimensional dependence of χ^2 on the temperature ([parameter_errors-temp_spectrum.dat](#)). The picture of these data sets is stored in the output file [parameter_errors_spectrum.png](#) and shown here in Figure 6.6d. In this figure, the uncertainty ranges of the fitting parameters are depicted in dark red, and the optimized values of the fitting parameters are depicted by white dots. As expected, all dots appear within the uncertainty ranges mentioned above, meaning that the optimized values of the fitting parameters lay within the corresponding uncertainty ranges. In order to determine the errors of fitting parameters, all three two-dimensional dependencies from Figure 6.6d were transformed into one-dimensional dependencies, which contain the dependence of χ^2 on each single fitting parameter. The one-dimensional dependencies are stored in the output file [confidence_intervals_spectrum.png](#), whose content is depicted in Figure 6.6e. As can be seen, all one-dimensional dependencies reveal a single, well-defined minimum. The χ^2 threshold, which was used to determine the uncertainty intervals of the fitting parameters, is depicted by the black dashed line. The errors of individual fitting parameters, which were derived from the uncertainty intervals, are listed Figure 6.6c. The errors of the mean inter-spin distance $\langle r \rangle$ and its standard deviation Δr are ± 0.02 nm and ± 0.03 nm, respectively. The error of both angular parameters, $\langle \xi \rangle$ and $\Delta \xi$, is $\pm 1^\circ$. Thus, both distributions, $P(r)$ and $P(\xi)$, could be extracted from the RIDME spectrum of Q8R1 with a very high precision. The optimized value of the temperature equals to 2.2 ± 0.2 K. This value deviates from the experimental temperature (3 K)^[5] by 1.0 ± 0.3 K. The obtained deviation is in agreement with the reported experimental error of the temperature measurement (~ 1 K).^[5]

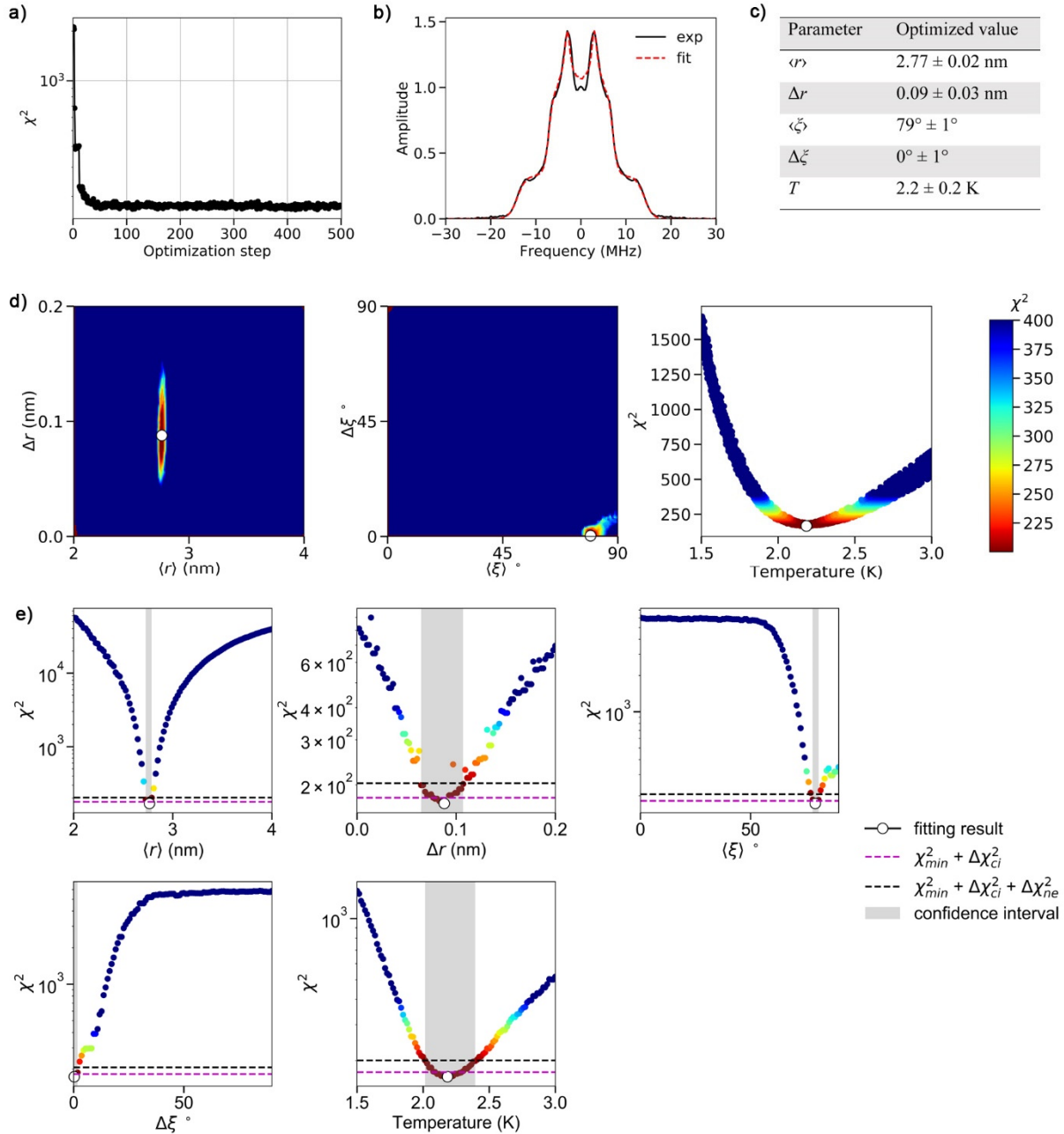


Figure 6.6. Fitting the RIDME spectrum of Q8R1 by AnisoDipFit. **a)** The dependence of χ^2 on the optimization step. **b)** The RIDME spectrum (black line) is overlaid with the corresponding fit (red line). **c)** The optimized values of the fitting parameters. **d)** The dependence of χ^2 on different pairs of fitting parameters. Dark red regions correspond to the parameters' uncertainty intervals, which lie below the χ^2 threshold. The optimized values of the fitting parameters are depicted by white dots. **e)** The dependence of χ^2 on single fitting parameters. The χ^2 threshold is depicted by the black dashed line. This threshold consists of two contributions, $\Delta\chi^2_{ci}$, which is determined at the 3σ confidence level, and $\Delta\chi^2_{ne}$, which takes into account the numerical error. The uncertainty ranges of the fitting parameters are shown as gray intervals.

7 References

- [1] P. P. Borbat, J. H. Freed, *eMagRes* **2017**, *6*, 465–494.
- [2] G. Jeschke, *eMagRes* **2016**, *5*, 1459–1476.
- [3] G. Jeschke, V. Chechik, P. Ionita, A. Godt, H. Zimmermann, J. Banham, C. R. Timmel, D. Hilger, H. Jung, *Appl. Magn. Reson.* **2006**, *30*, 473–498.
- [4] A. F. Bedilo, A. G. Maryasov, *J. Magn. Reson.* **1995**, *116*, 87–96.
- [5] D. Abdullin, H. Matsuoka, M. Yulikov, N. Fleck, C. Klein, S. Spicher, G. Hagelueken, S. Grimme, A. Luetzen, O. Schiemann, *Chem. Eur. J.* **2019**, *25*, 8820–8828.
- [6] D. Abdullin, P. Brehm, N. Fleck, S. Spicher, S. Grimme, O. Schiemann, *Chem. – A Eur. J.* **2019**, *25*, 14388–14398.
- [7] D. Abdullin, *Appl. Magn. Reson.* **2020**, *51*, 725–748.
- [8] B. Filipič, J. Štrancar, *Appl. Soft Comput.* **2001**, *1*, 83–90.
- [9] T. Spałek, P. Pietrzyk, Z. Sojka, *J. Chem. Inf. Model.* **2005**, *45*, 18–29.
- [10] S. Stoll, A. Schweiger, *J. Magn. Reson.* **2006**, *178*, 42–55.
- [11] D. Abdullin, G. Hagelueken, R. I. Hunter, G. M. Smith, O. Schiemann, *Mol. Phys.* **2015**, *113*, 544–560.
- [12] W. H. Press, S. A. Teukolsky, W. T. Vetterling, B. P. Flannery, *Numerical Recipes in C*, Cambridge University Press, Cambridge, **1992**.
- [13] T. H. Edwards, S. Stoll, *J. Magn. Reson.* **2016**, *270*, 87–97.
- [14] O. Schiemann, T. F. Prisner, *Q. Rev. Biophys.* **2007**, *40*, 1–53.
- [15] L. V. Kulik, S. A. Dzuba, I. A. Grigoryev, Y. D. Tsvetkov, *Chem. Phys. Lett.* **2001**, *343*, 315–324.
- [16] S. Milikisyants, F. Scarpelli, M. G. Finiguerra, M. Ubbink, M. Huber, *J. Magn. Reson.* **2009**, *201*, 48–56.
- [17] M. Fittipaldi, I. García-Rubio, F. Trandafir, I. Gromov, A. Schweiger, A. Bouwen, S. Van Doorslaer, *J. Phys. Chem. B* **2008**, *112*, 3859–3870.
- [18] R. Maurus, C. M. Overall, R. Bogumil, Y. Luo, A. G. Mauk, M. Smith, G. D. Brayer, *Biochim. Biophys. Acta, Protein Struct. Mol. Enzymol.* **1997**, *1341*, 1–13.